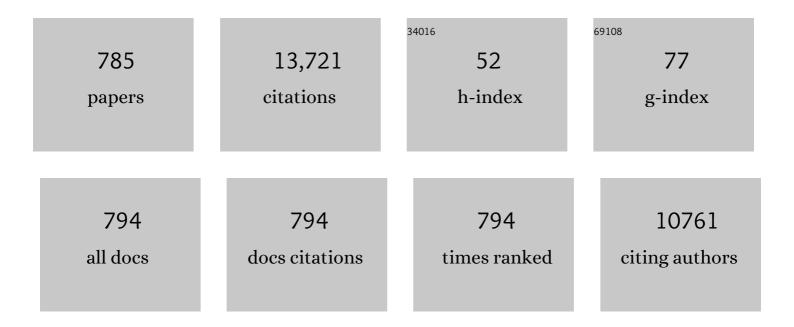
Eduardo Alves

List of Publications by Year in descending order

Source: https://exaly.com/author-pdf/7484251/publications.pdf Version: 2024-02-01



FOUNDO AIVES

#	Article	IF	CITATIONS
1	Effect of post-annealing on the properties of copper oxide thin films obtained from the oxidation of evaporated metallic copper. Applied Surface Science, 2008, 254, 3949-3954.	3.1	226
2	Strain and composition distributions in wurtzite InGaN/GaN layers extracted from x-ray reciprocal space mapping. Applied Physics Letters, 2002, 80, 3913-3915.	1.5	209
3	Characterisation of Ti1â^'xSixNy nanocomposite films. Surface and Coatings Technology, 2000, 133-134, 307-313.	2.2	190
4	Compositional pulling effects inInxGa1â^'xN/GaNlayers: A combined depth-resolved cathodoluminescence and Rutherford backscattering/channeling study. Physical Review B, 2001, 64, .	1.1	176
5	Structural, optical and mechanical properties of coloured TiNxOy thin films. Thin Solid Films, 2004, 447-448, 449-454.	0.8	169
6	Overview of the JET results in support to ITER. Nuclear Fusion, 2017, 57, 102001.	1.6	150
7	Influence of nitrogen content on the structural, mechanical and electrical properties of TiN thin films. Surface and Coatings Technology, 2005, 191, 317-323.	2.2	146
8	Microstructure and mechanical properties of nanocomposite (Ti,Si,Al)N coatings. Thin Solid Films, 2001, 398-399, 391-396.	0.8	131
9	Anomalous Ion Channeling inAlInN/GaNBilayers: Determination of the Strain State. Physical Review Letters, 2006, 97, 085501.	2.9	125
10	Metal-organic vapor phase epitaxy and properties of AlInN in the whole compositional range. Applied Physics Letters, 2007, 90, 022105.	1.5	119
11	Materials design data for reduced activation martensitic steel type EUROFER. Journal of Nuclear Materials, 2004, 329-333, 257-262.	1.3	118
12	Hard nanocomposite Ti–Si–N coatings prepared by DC reactive magnetron sputtering. Surface and Coatings Technology, 2000, 133-134, 234-239.	2.2	115
13	Compositional dependence of the strain-free optical band gap in InxGa1â^'xN layers. Applied Physics Letters, 2001, 78, 2137-2139.	1.5	104
14	Damage formation and annealing at low temperatures in ion implanted ZnO. Applied Physics Letters, 2005, 87, 191904.	1.5	100
15	Structural and optical properties of InGaN/GaN layers close to the critical layer thickness. Applied Physics Letters, 2002, 81, 1207-1209.	1.5	94
16	Photoluminescence and lattice location of Eu and Pr implanted GaN samples. Physica B: Condensed Matter, 2001, 308-310, 22-25.	1.3	91
17	Identification of the prime optical center in <mml:math xmlns:mml="http://www.w3.org/1998/Math/MathML" display="inline"><mml:mrow><mml:mtext>GaN</mml:mtext><mml:mo>:</mml:mo><mml:msup><mml:mrow Physical Review B. 2010. 81</mml:mrow </mml:msup></mml:mrow></mml:math 	> < mml:mte	ext>20
18	Structural, electrical, optical, and mechanical characterizations of decorative ZrOxNy thin films. Journal of Applied Physics, 2005, 98, 023715.	1.1	87

#	Article	IF	CITATIONS
19	Overview of the JET preparation for deuterium–tritium operation with the ITER like-wall. Nuclear Fusion, 2019, 59, 112021.	1.6	87
20	Direct Evidence for As as a Zn-Site Impurity in ZnO. Physical Review Letters, 2005, 95, 215503.	2.9	86
21	Selectively excited photoluminescence from Eu-implanted GaN. Applied Physics Letters, 2005, 87, 112107.	1.5	85
22	Photoluminescence studies in ZnO samples. Physica B: Condensed Matter, 2001, 308-310, 985-988.	1.3	84
23	Effects of ion bombardment on properties of d.c. sputtered superhard (Ti, Si, Al)N nanocomposite coatings. Surface and Coatings Technology, 2002, 151-152, 515-520.	2.2	81
24	Synthesis, surface modification and optical properties of Tb3+-doped ZnO nanocrystals. Nanotechnology, 2006, 17, 834-839.	1.3	75
25	Material migration patterns and overview of first surface analysis of the JET ITER-like wall. Physica Scripta, 2014, T159, 014010.	1.2	75
26	Plasma–wall interaction studies within the EUROfusion consortium: progress on plasma-facing components development and qualification. Nuclear Fusion, 2017, 57, 116041.	1.6	75
27	Preparation of magnetron sputtered TiNxOy thin films. Surface and Coatings Technology, 2003, 174-175, 197-203.	2.2	74
28	Tuning of the surface plasmon resonance in TiO2/Au thin films grown by magnetron sputtering: The effect of thermal annealing. Journal of Applied Physics, 2011, 109, .	1.1	74
29	Implantation damage formation in a-, c- and m-plane GaN. Acta Materialia, 2017, 123, 177-187.	3.8	73
30	Three-step amorphisation process in ion-implanted GaN at 15 K. Nuclear Instruments & Methods in Physics Research B, 2003, 206, 1028-1032.	0.6	71
31	Characterization of TiAlSiN/TiAlSiON/SiO2 optical stack designed by modelling calculations for solar selective applications. Solar Energy Materials and Solar Cells, 2012, 105, 202-207.	3.0	70
32	Solar selective absorbers based on Al2O3:W cermets and AlSiN/AlSiON layers. Solar Energy Materials and Solar Cells, 2015, 137, 93-100.	3.0	68
33	High-temperature annealing and optical activation of Eu-implanted GaN. Applied Physics Letters, 2004, 85, 2712-2714.	1.5	67
34	Electrical, structural and optical characterization of copper oxide thin films as a function of post annealing temperature. Physica Status Solidi (A) Applications and Materials Science, 2009, 206, 2143-2148.	0.8	67
35	Lattice site location and optical activity of Er implanted ZnO. Nuclear Instruments & Methods in Physics Research B, 2003, 206, 1047-1051.	0.6	66
36	Influence of the chemical and electronic structure on the electrical behavior of zirconium oxynitride films. Journal of Applied Physics, 2008, 103, .	1.1	66

#	Article	lF	CITATIONS
37	High Orbital Angular Momentum Harmonic Generation. Physical Review Letters, 2016, 117, 265001.	2.9	66
38	Micron-scale analysis of SiC/SiCf composites using the new Lisbon nuclear microprobe. Nuclear Instruments & Methods in Physics Research B, 2000, 161-163, 334-338.	0.6	65
39	Property change in ZrNxOy thin films: effect of the oxygen fraction and bias voltage. Thin Solid Films, 2004, 469-470, 11-17.	0.8	65
40	Efficient dipole-dipole coupling of Mott-Wannier and Frenkel excitons in (Ga,In)N quantum well/polyfluorene semiconductor heterostructures. Physical Review B, 2007, 76, .	1.1	64
41	Radiation damage in ZnO ion implanted at 15K. Nuclear Instruments & Methods in Physics Research B, 2009, 267, 2708-2711.	0.6	64
42	Role of Nanoscale Strain Inhomogeneity on the Light Emission from InGaN Epilayers. Advanced Functional Materials, 2007, 17, 37-42.	7.8	60
43	Identification of donor-related impurities in ZnO using photoluminescence and radiotracer techniques. Physical Review B, 2006, 73, .	1.1	59
44	An overview of the comprehensive First Mirror Test in JET with ITER-like wall. Physica Scripta, 2014, T159, 014011.	1.2	59
45	Dielectric function of nanocrystalline silicon with few nanometers (<3 nm) grain size. Applied Physics Letters, 2003, 82, 2993-2995.	1.5	58
46	Application of RZ-scan technique for investigation of nonlinear refraction of sapphire doped with Ag, Cu, and Au nanoparticles. Optics Communications, 2005, 253, 205-213.	1.0	58
47	Transmission electron microscopy investigation of the structural damage formed in GaN by medium range energy rare earth ion implantation. Journal of Applied Physics, 2006, 100, 073520.	1.1	58
48	Optical energies of AlInN epilayers. Journal of Applied Physics, 2008, 103, .	1.1	58
49	Photoluminescence and damage recovery studies in Fe-implanted ZnO single crystals. Journal of Applied Physics, 2003, 93, 8995-9000.	1.1	56
50	Interpretation of double x-ray diffraction peaks from InGaN layers. Applied Physics Letters, 2001, 79, 1432-1434.	1.5	55
51	Implantation site of rare earths in single-crystalline ZnO. Applied Physics Letters, 2003, 82, 1173-1175.	1.5	55
52	Near-band-edge slow luminescence in nominally undoped bulk ZnO. Journal of Applied Physics, 2005, 98, 013502.	1.1	54
53	Radiation damage formation and annealing in GaN and ZnO. Proceedings of SPIE, 2011, , .	0.8	54
54	Optimization of nanocomposite Au/TiO 2 thin films towards LSPR optical-sensing. Applied Surface Science, 2018, 438, 74-83.	3.1	54

#	Article	IF	CITATIONS
55	Ion beam analysis of fusion plasma-facing materials and components: facilities and research challenges. Nuclear Fusion, 2020, 60, 025001.	1.6	54
56	Raman study of the A1(LO) phonon in relaxed and pseudomorphic InGaN epilayers. Applied Physics Letters, 2003, 83, 4761-4763.	1.5	53
57	Optical studies of ZnO nanocrystals doped with Eu3+ ions. Applied Physics A: Materials Science and Processing, 2007, 88, 129-133.	1.1	53
58	Corrosion resistance of ZrNxOy thin films obtained by rf reactive magnetron sputtering. Thin Solid Films, 2004, 469-470, 274-281.	0.8	52
59	Microstructure of (Ti,Si,Al)N nanocomposite coatings. Surface and Coatings Technology, 2004, 177-178, 369-375.	2.2	52
60	High Mobility a-IGO Films Produced at Room Temperature and Their Application in TFTs. Electrochemical and Solid-State Letters, 2010, 13, H20.	2.2	52
61	Identifying the influence of the intrinsic defects in Gd-doped ZnO thin-films. Journal of Applied Physics, 2016, 119, .	1.1	52
62	Long-term fuel retention in JET ITER-like wall. Physica Scripta, 2016, T167, 014075.	1.2	52
63	Overview of JET results for optimising ITER operation. Nuclear Fusion, 2022, 62, 042026.	1.6	52
64	Lattice location and thermal stability of implanted Fe in ZnO. Applied Physics Letters, 2004, 85, 4899-4901.	1.5	50
65	Relaxation of compressively strained AlInN on GaN. Journal of Crystal Growth, 2008, 310, 4058-4064.	0.7	50
66	Fuel retention in JET ITER-Like Wall from post-mortem analysis. Journal of Nuclear Materials, 2015, 463, 961-965.	1.3	50
67	The influence of annealing treatments on the properties of Ag:TiO2 nanocomposite films prepared by magnetron sputtering. Applied Surface Science, 2012, 258, 4028-4034.	3.1	49
68	Transparent thin film transistors based on indium oxide semiconductor. Journal of Non-Crystalline Solids, 2006, 352, 2311-2314.	1.5	48
69	PVD-Grown photocatalytic TiO2 thin films on PVDF substrates for sensors and actuators applications. Thin Solid Films, 2008, 517, 1161-1166.	0.8	48
70	Structural and optical characterization of Eu-implanted GaN. Journal Physics D: Applied Physics, 2009, 42, 165103.	1.3	48
71	Global erosion and deposition patterns in JET with the ITER-like wall. Journal of Nuclear Materials, 2015, 463, 157-161.	1.3	48
72	High temperature annealing of rare earth implanted GaN films: Structural and optical properties. Optical Materials, 2006, 28, 750-758.	1.7	47

#	Article	IF	CITATIONS
73	Overview of fuel inventory in JET with the ITER-like wall. Nuclear Fusion, 2017, 57, 086045.	1.6	47
74	Structural evolution in ZrNxOy thin films as a function of temperature. Surface and Coatings Technology, 2006, 200, 2917-2922.	2.2	46
75	Overview of the JET ITER-like wall divertor. Nuclear Materials and Energy, 2017, 12, 499-505.	0.6	46
76	Elastic properties of (Ti,Al,Si)N nanocomposite films. Surface and Coatings Technology, 2001, 142-144, 110-116.	2.2	45
77	Hydrogenated silicon carbon nitride films obtained by HWCVD, PA-HWCVD and PECVD techniques. Journal of Non-Crystalline Solids, 2006, 352, 1361-1366.	1.5	45
78	Direct observation of mono-vacancy and self-interstitial recovery in tungsten. APL Materials, 2019, 7, .	2.2	45
79	Lattice location and optical activation of rare earth implanted GaN. Materials Science and Engineering B: Solid-State Materials for Advanced Technology, 2003, 105, 132-140.	1.7	44
80	Mechanical characterization of reactively magnetron-sputtered TiN films. Surface and Coatings Technology, 2003, 174-175, 375-382.	2.2	44
81	Functional and optical properties of Au:TiO2 nanocomposite films: The influence of thermal annealing. Applied Surface Science, 2010, 256, 6536-6542.	3.1	43
82	Room-temperature growth of crystalline indium tin oxide films on glass using low-energy oxygen-ion-beam assisted deposition. Journal of Applied Physics, 2003, 93, 2262-2266.	1.1	42
83	Free electron behavior in InN: On the role of dislocations and surface electron accumulation. Applied Physics Letters, 2009, 94, 022109.	1.5	41
84	Lattice location and stability of implanted Cu in ZnO. Physical Review B, 2004, 69, .	1.1	40
85	The role of composition, morphology and crystalline structure in the electrochemical behaviour of TiNx thin films for dry electrode sensor materials. Electrochimica Acta, 2009, 55, 59-67.	2.6	40
86	Optical and structural analysis of solar selective absorbing coatings based on AlSiOx:W cermets. Solar Energy, 2017, 150, 335-344.	2.9	40
87	Cathodoluminescence of rare earth implanted Ga2O3and GeO2nanostructures. Nanotechnology, 2011, 22, 285706.	1.3	39
88	Mechanisms of damage formation in Eu-implanted GaN probed by X-ray diffraction. Europhysics Letters, 2011, 96, 46002.	0.7	39
89	Efficient temperature sensing using photoluminescence of Er/Yb implanted GaN thin films. Sensors and Actuators B: Chemical, 2017, 248, 769-776.	4.0	39
90	Structural and corrosion behaviour of stoichiometric and substoichiometric TiN thin films. Surface and Coatings Technology, 2004, 180-181, 158-163.	2.2	38

#	Article	IF	CITATIONS
91	Raman spectra and structural analysis in ZrOxNy thin films. Thin Solid Films, 2006, 515, 1132-1137.	0.8	38
92	Optically active centers in Eu implanted, Euin situdoped GaN, and Eu doped GaN quantum dots. Journal of Applied Physics, 2009, 105, 043104.	1.1	38
93	Optical doping and damage formation in AlN by Eu implantation. Journal of Applied Physics, 2010, 107, 023525.	1.1	38
94	Nanocomposite Ag:TiN thin films for dry biopotential electrodes. Applied Surface Science, 2013, 285, 40-48.	3.1	38
95	Structural and luminescence properties of Eu and Er implanted Bi2O3 nanowires for optoelectronic applications. Journal of Materials Chemistry C, 2013, 1, 7920.	2.7	38
96	A design of selective solar absorber for high temperature applications. Solar Energy, 2018, 172, 177-183.	2.9	38
97	Enhancement in the photocatalytic nature of nitrogen-doped PVD-grown titanium dioxide thin films. Journal of Applied Physics, 2009, 106, .	1.1	37
98	TiNx coated polycarbonate for bio-electrode applications. Corrosion Science, 2012, 56, 49-57.	3.0	37
99	Ion beam studies of TiNxOy thin films deposited by reactive magnetron sputtering. Surface and Coatings Technology, 2004, 180-181, 372-376.	2.2	36
100	Characterization of hard DC-sputtered Si-based TiN coatings: the effect of composition and ion bombardment. Surface and Coatings Technology, 2004, 188-189, 351-357.	2.2	36
101	Structural evolution of Ti–Al–Si–N nanocomposite coatings. Vacuum, 2009, 83, 1206-1212.	1.6	36
102	Hydrogen in InN: A ubiquitous phenomenon in molecular beam epitaxy grown material. Applied Physics Letters, 2010, 96, .	1.5	36
103	High In-content InGaN layers synthesized by plasma-assisted molecular-beam epitaxy: Growth conditions, strain relaxation, and In incorporation kinetics. Journal of Applied Physics, 2014, 116, .	1.1	36
104	Surface analysis of tiles and samples exposed to the first JET campaigns with the ITER-like wall. Physica Scripta, 2014, T159, 014012.	1.2	35
105	Neutron spectroscopy measurements of 14 MeV neutrons at unprecedented energy resolution and implications for deuterium–tritium fusion plasma diagnostics. Measurement Science and Technology, 2018, 29, 045502.	1.4	35
106	Green, red and infrared Er-related emission in implanted GaN:Er and GaN:Er,O samples. Journal of Applied Physics, 2001, 89, 6183-6188.	1.1	34
107	TiAgx thin films for lower limb prosthesis pressure sensors: Effect of composition and structural changes on the electrical and thermal response of the films. Applied Surface Science, 2013, 285, 10-18.	3.1	34
108	p-Type <formula formulatype="inline"><tex Notation="TeX">\${hbox{Cu}}_{x}{hbox{O}}\$ </tex </formula> Thin-Film Transistors Produced by Thermal Oxidation. Journal of Display Technology, 2013, 9, 735-740.	1.3	34

#	Article	IF	CITATIONS
109	Comparison of low- and room-temperature damage formation in Ar ion implanted GaN and ZnO. Nuclear Instruments & Methods in Physics Research B, 2013, 307, 394-398.	0.6	34
110	OPTICAL DOPING OF NITRIDES BY ION IMPLANTATION. Modern Physics Letters B, 2001, 15, 1281-1287.	1.0	33
111	Depth-resolved analysis of spontaneous phase separation in the growth of lattice-matched AlInN. Journal Physics D: Applied Physics, 2010, 43, 055406.	1.3	33
112	Rapid thermal annealing of rare earth implanted ZnO epitaxial layers. Optical Materials, 2011, 33, 1139-1142.	1.7	33
113	Properties of tantalum oxynitride thin films produced by magnetron sputtering: The influence of processing parameters. Vacuum, 2013, 98, 63-69.	1.6	33
114	Mechanisms of Implantation Damage Formation in Al _{<i>x</i>} Ga _{1–<i>x</i>} N Compounds. Journal of Physical Chemistry C, 2016, 120, 7277-7283.	1.5	33
115	Tribocorrosion behaviour of ZrOxNy thin films for decorative applications. Surface and Coatings Technology, 2006, 200, 6634-6639.	2.2	32
116	Deuterium retention in tin (Sn) and lithium–tin (Li–Sn) samples exposed to ISTTOK plasmas. Nuclear Materials and Energy, 2017, 12, 709-713.	0.6	32
117	Luminescence of Eu ions in <mml:math <br="" xmlns:mml="http://www.w3.org/1998/Math/MathML">display="inline"><mml:mrow><mml:msub><mml:mrow><mml:mtext>Al</mml:mtext></mml:mrow><mml:mi>x the entire alloy composition range. Physical Review B, 2009, 80, .</mml:mi></mml:msub></mml:mrow></mml:math>		⊳aml:msub>
118	Consolidation of W–Ta composites: Hot isostatic pressing and spark and pulse plasma sintering. Fusion Engineering and Design, 2015, 98-99, 1950-1955.	1.0	31
119	Substrate effect on CdTe layers grown by metalorganic vapor phase epitaxy. Applied Physics Letters, 1997, 70, 1314-1316.	1.5	30
120	Optical doping of ZnO with Tm by ion implantation. Physica B: Condensed Matter, 2003, 340-342, 235-239.	1.3	30
121	Roughness in GaN/InGaN films and multilayers determined with Rutherford backscattering. Nuclear Instruments & Methods in Physics Research B, 2004, 217, 479-497.	0.6	30
122	First results and surface analysis strategy for plasma-facing components after JET operation with the ITER-like wall. Physica Scripta, 2014, T159, 014016.	1.2	30
123	Electrochemical behaviour of nanocomposite Agx:TiN thin films for dry biopotential electrodes. Electrochimica Acta, 2014, 125, 48-57.	2.6	30
124	Thin films of Ag–Au nanoparticles dispersed in TiO ₂ : influence of composition and microstructure on the LSPR and SERS responses. Journal Physics D: Applied Physics, 2018, 51, 205102.	1.3	30
125	Effect of annealing temperature on luminescence in Eu implanted GaN. Optical Materials, 2006, 28, 780-784.	1.7	29
126	Visible and infrared luminescence study of Er doped β-Ga ₂ O ₃ and Er ₃ Ga ₅ O ₁₂ . Journal Physics D: Applied Physics, 2008, 41, 065406.	1.3	29

#	Article	IF	CITATIONS
127	Lattice site location of optical centers in GaN:Eu light emitting diode material grown by organometallic vapor phase epitaxy. Applied Physics Letters, 2010, 97, 111911.	1.5	29
128	Single phase a-plane MgZnO epilayers for UV optoelectronics: substitutional behaviour of Mg at large contents. CrystEngComm, 2012, 14, 1637-1640.	1.3	29
129	Study of the relationship between crystal structure and luminescence in rare-earth-implanted Ga2O3 nanowires during annealing treatments. Journal of Materials Science, 2014, 49, 1279-1285.	1.7	29
130	Utilization of native oxygen in Eu(RE)-doped GaN for enabling device compatibility in optoelectronic applications. Scientific Reports, 2016, 6, 18808.	1.6	29
131	Incorporation and stability of erbium in sapphire by ion implantation. Nuclear Instruments & Methods in Physics Research B, 1995, 106, 429-432.	0.6	28
132	Comparative study of radiation damage in GaN and InGaN by 400 keV Au implantation. Nuclear Instruments & Methods in Physics Research B, 2004, 218, 36-41.	0.6	28
133	Tribological behaviour of Cl-implanted TiN coatings for biomedical applications. Wear, 2007, 262, 1337-1345.	1.5	28
134	Influence of the O/C ratio in the behaviour of TiCxOy thin films. Surface and Coatings Technology, 2007, 201, 5587-5591.	2.2	28
135	Optical properties of LFZ grown β-Ga2O3:Eu3+ fibres. Applied Surface Science, 2012, 258, 9157-9161.	3.1	28
136	Intense luminescence emission from rare-earth-doped MoO3nanoplates and lamellar crystals for optoelectronic applications. Journal Physics D: Applied Physics, 2014, 47, 355105.	1.3	28
137	Assessment of erosion, deposition and fuel retention in the JET-ILW divertor from ion beam analysis data. Nuclear Materials and Energy, 2017, 12, 559-563.	0.6	28
138	Amorphisation of GaN during processing with rare earth ion beams. Superlattices and Microstructures, 2004, 36, 737-745.	1.4	27
139	Structural stability of decorative ZrNxOy thin films. Surface and Coatings Technology, 2005, 200, 748-752.	2.2	27
140	Defect production in neutron irradiated GaN. Nuclear Instruments & Methods in Physics Research B, 2006, 249, 358-361.	0.6	27
141	Indium kinetics during the plasma-assisted molecular beam epitaxy of semipolar (11â^22) InGaN layers. Applied Physics Letters, 2010, 96, 181907.	1.5	27
142	Colossal dielectric constant of poly- and single-crystalline CaCu3Ti4O12 fibres grown by the laser floating zone technique. Acta Materialia, 2011, 59, 102-111.	3.8	27
143	The photoluminescence/excitation (PL/E) spectroscopy of Eu-implanted GaN. Optical Materials, 2011, 33, 1063-1065.	1.7	27
144	Analysis of multifunctional titanium oxycarbide films as a function of oxygen addition. Surface and Coatings Technology, 2012, 206, 2525-2534.	2.2	27

#	Article	IF	CITATIONS
145	Ag:TiNâ€Coated Polyurethane for Dry Biopotential Electrodes: From Polymer Plasma Interface Activation to the First EEG Measurements. Plasma Processes and Polymers, 2016, 13, 341-354.	1.6	27
146	Lattice site and photoluminescence of erbium implanted in α–Al ₂ O ₃ . Journal of Materials Research, 1997, 12, 1401-1404.	1.2	26
147	Ion beam and photoluminescence studies of Er and O implanted GaN. Nuclear Instruments & Methods in Physics Research B, 1999, 147, 383-387.	0.6	26
148	Resonant Raman scattering in ZnO:Mn and ZnO:Mn:Al thin films grown by RF sputtering. Journal of Physics Condensed Matter, 2011, 23, 334205.	0.7	26
149	Experience on divertor fuel retention after two ITER-Like Wall campaigns. Physica Scripta, 2017, T170, 014063.	1.2	26
150	Doping β-Ga ₂ O ₃ with europium: influence of the implantation and annealing temperature. Journal Physics D: Applied Physics, 2017, 50, 325101.	1.3	26
151	Compositional analysis by RBS, XPS and EDX of ZnO:Al,Bi and ZnO:Ga,Bi thin films deposited by d.c. magnetron sputtering. Vacuum, 2019, 161, 268-275.	1.6	26
152	Unravelling the secrets of the resistance of GaN to strongly ionising radiation. Communications Physics, 2021, 4, .	2.0	26
153	Luminescence and structural studies of iron implanted α-Al2O3. Nuclear Instruments & Methods in Physics Research B, 2002, 191, 638-643.	0.6	25
154	Up conversion from visible to ultraviolet in bulk ZnO implanted with Tm ions. Applied Physics Letters, 2005, 87, 192108.	1.5	25
155	A green-emitting CdSe/poly(butyl acrylate) nanocomposite. Nanotechnology, 2005, 16, 1969-1973.	1.3	25
156	Stability and luminescence studies of Tm and Er implanted ZnO single crystals. Nuclear Instruments & Methods in Physics Research B, 2006, 242, 580-584.	0.6	25
157	Optical and structural analysis of bulk ZnO samples undoped and rare earth doped by ion implantation. Superlattices and Microstructures, 2006, 39, 202-210.	1.4	25
158	Raman and XRD studies of Ge nanocrystals in alumina films grown by RF-magnetron sputtering. Vacuum, 2008, 82, 1466-1469.	1.6	25
159	Fuel inventory and deposition in castellated structures in JET-ILW. Nuclear Fusion, 2017, 57, 066027.	1.6	25
160	Fe ion implantation in GaN: Damage, annealing, and lattice site location. Journal of Applied Physics, 2001, 90, 81-86.	1.1	24
161	Microstructural studies of PZT thick films on Cu foils. Acta Materialia, 2006, 54, 3211-3220.	3.8	24
162	Structural and electrical properties of Al doped ZnO thin films deposited at room temperature on poly(vinilidene fluoride) substrates. Thin Solid Films, 2009, 517, 6290-6293.	0.8	24

#	Article	IF	CITATIONS
163	ZrO _{<i>x</i>} N _{<i>y</i>} decorative thin films prepared by the reactive gas pulsing process. Journal Physics D: Applied Physics, 2009, 42, 195501.	1.3	24
164	Comparison of radiation detector performance for different metal contacts on CdZnTe deposited by electroless deposition method. Crystal Research and Technology, 2011, 46, 1131-1136.	0.6	24
165	Electrical properties of AlNxOy thin films prepared by reactive magnetron sputtering. Thin Solid Films, 2012, 520, 6709-6717.	0.8	24
166	Influence of stoichiometry and structure on the optical properties of AlN _x O _y films. Journal Physics D: Applied Physics, 2013, 46, 015305.	1.3	24
167	Determination of the 9Be(3He,pi)11B (i=0,1,2,3) cross section at 135° in the energy range 1–2.5MeV. Nuclear Instruments & Methods in Physics Research B, 2015, 346, 21-25.	0.6	24
168	Thin films composed of Au nanoparticles embedded in AlN: Influence of metal concentration and thermal annealing on the LSPR band. Vacuum, 2018, 157, 414-421.	1.6	24
169	First mirror test in JET for ITER: Complete overview after three ILW campaigns. Nuclear Materials and Energy, 2019, 19, 59-66.	0.6	24
170	Photoelectrochemical Water Splitting: Thermal Annealing Challenges on Hematite Nanowires. Journal of Physical Chemistry C, 2020, 124, 12897-12911.	1.5	24
171	Structural and magnetic studies of Fe-implanted α-Al2O3. Surface and Coatings Technology, 2000, 128-129, 434-439.	2.2	23
172	Conductivity behaviour of Cr implanted TiO2. Nuclear Instruments & Methods in Physics Research B, 2002, 191, 158-162.	0.6	23
173	Lattice site and stability of implanted Ag in ZnO. Physica B: Condensed Matter, 2003, 340-342, 240-244.	1.3	23
174	Detection angle resolved PIXE and the equivalent depth concept for thin film characterization. X-Ray Spectrometry, 2005, 34, 372-375.	0.9	23
175	Optical doping of AlN by rare earth implantation. Nuclear Instruments & Methods in Physics Research B, 2006, 242, 307-310.	0.6	23
176	Accurate simulation of backscattering spectra in the presence of sharp resonances. Nuclear Instruments & Methods in Physics Research B, 2006, 247, 381-389.	0.6	23
177	High pressure annealing of Europium implanted GaN. Proceedings of SPIE, 2012, , .	0.8	23
178	Laser-assisted cleaning of beryllium-containing mirror samples from JET and PISCES-B. Fusion Engineering and Design, 2014, 89, 122-130.	1.0	23
179	Zr-O-N coatings for decorative purposes: Study of the system stability by exploration of the deposition parameter space. Surface and Coatings Technology, 2018, 343, 30-37.	2.2	23
180	Deposition of impurity metals during campaigns with the JET ITER-like Wall. Nuclear Materials and Energy, 2019, 19, 218-224.	0.6	23

#	Article	IF	CITATIONS
181	Annealing behavior and lattice site location of Hf implanted GaN. Materials Science and Engineering B: Solid-State Materials for Advanced Technology, 1999, 59, 207-210.	1.7	22
182	RBS/Channeling study of Er doped GaN films grown by MBE on Si substrates. Nuclear Instruments & Methods in Physics Research B, 2000, 161-163, 946-951.	0.6	22
183	Anisotropic electrical transport in epitaxial La2/3Ca1/3MnO3 thin films. Journal of Applied Physics, 2000, 87, 5570-5572.	1.1	22
184	Electrical conductivity of MgO crystals implanted with lithium ions. Nuclear Instruments & Methods in Physics Research B, 2002, 191, 191-195.	0.6	22
185	Properties of MoNxOy thin films as a function of the N/O ratio. Thin Solid Films, 2006, 494, 201-206.	0.8	22
186	Further insight into the temperature quenching of photoluminescence from InAsâ^•GaAs self-assembled quantum dots. Journal of Applied Physics, 2008, 103, .	1.1	22
187	Room-Temperature Cosputtered HfO[sub 2]–Al[sub 2]O[sub 3] Multicomponent Gate Dielectrics. Electrochemical and Solid-State Letters, 2009, 12, G65.	2.2	22
188	Enhanced red emission from praseodymium-doped GaN nanowires by defect engineering. Acta Materialia, 2013, 61, 3278-3284.	3.8	22
189	Evolution of the mechanical properties of Ti-based intermetallic thin films doped with different metals to be used as biomedical devices. Applied Surface Science, 2020, 505, 144617.	3.1	22
190	Etching of amorphous Al2O3 produced by ion implantation. Nuclear Instruments & Methods in Physics Research B, 1997, 127-128, 596-598.	0.6	21
191	Physical and morphological characterization of reactively magnetron sputtered TiN films. Thin Solid Films, 2002, 420-421, 421-428.	0.8	21
192	Effects of the morphology and structure on the elastic behavior of (Ti,Si,Al)N nanocomposites. Surface and Coatings Technology, 2003, 174-175, 984-991.	2.2	21
193	Direct evidence for strain inhomogeneity in InxGa1â ^{^,} xN epilayers by Raman spectroscopy. Applied Physics Letters, 2004, 85, 2235-2237.	1.5	21
194	Microstructural characterization of Eurofer-ODS RAFM steel in the normalized and tempered condition and after thermal aging in simulated fusion conditions. Fusion Engineering and Design, 2005, 75-79, 1061-1065.	1.0	21
195	Nonlinear optical properties of gold nanoparticles synthesized by ion implantation in sapphire matrix. Technical Physics Letters, 2005, 31, 702-705.	0.2	21
196	Structural anisotropy of nonpolar and semipolar InN epitaxial layers. Journal of Applied Physics, 2010, 108, .	1.1	21
197	Structural and thermal characterization of SiO2–P2O5 sol–gel powders upon annealing at high temperatures. Journal of Non-Crystalline Solids, 2010, 356, 495-501.	1.5	21
198	Synergistic helium and deuterium blistering in tungsten–tantalum composites. Journal of Nuclear Materials, 2013, 442, 69-74.	1.3	21

#	Article	IF	CITATIONS
199	Determination of Ga auto-incorporation in nominal InAlN epilayers grown by MOCVD. Journal of Materials Chemistry C, 2014, 2, 5787.	2.7	21
200	Monte Carlo simulations of ion channeling in crystals containing dislocations and randomly displaced atoms. Journal of Applied Physics, 2019, 126, .	1.1	21
201	Microscopic studies of implanted 73As in diamond. Nuclear Instruments & Methods in Physics Research B, 1997, 127-128, 723-726.	0.6	20
202	A structural and mechanical analysis on PVD-grown (Ti,Al)N/Mo multilayers. Thin Solid Films, 2000, 377-378, 425-429.	0.8	20
203	Lattice location and annealing behavior of Mn implanted GaN. Nuclear Instruments & Methods in Physics Research B, 2002, 191, 544-548.	0.6	20
204	Splitting of X-ray diffraction and photoluminescence peaks in InGaN/GaN layers. Materials Science and Engineering B: Solid-State Materials for Advanced Technology, 2002, 93, 163-167.	1.7	20
205	Magnetic properties of TiO2 rutile implanted with Ni and Co. Journal of Magnetism and Magnetic Materials, 2005, 294, e73-e76.	1.0	20
206	Lattice sites of implanted Cu and Ag in ZnO. Superlattices and Microstructures, 2006, 39, 229-237.	1.4	20
207	Defect studies on fast and thermal neutron irradiated GaN. Nuclear Instruments & Methods in Physics Research B, 2008, 266, 2780-2783.	0.6	20
208	Single and polycrystalline mullite fibres grown by laser floating zone technique. Journal of the European Ceramic Society, 2010, 30, 3311-3318.	2.8	20
209	High Resolution and Differential PIXE combined with RBS, EBS and AFM analysis of magnesium titanate (MgTiO3) multilayer structures. Nuclear Instruments & Methods in Physics Research B, 2010, 268, 1980-1985.	0.6	20
210	Blistering of W–Ta composites at different irradiation energies. Journal of Nuclear Materials, 2013, 438, S1032-S1035.	1.3	20
211	Optimisation of surface treatments of TiO2:Nb transparent conductive coatings by a post-hot-wire annealing in a reducing H2 atmosphere. Thin Solid Films, 2014, 550, 404-412.	0.8	20
212	Multifunctional Ti–Me (Me=Al, Cu) thin film systems for biomedical sensing devices. Vacuum, 2015, 122, 353-359.	1.6	20
213	Biological behaviour of thin films consisting of Au nanoparticles dispersed in a TiO2 dielectric matrix. Vacuum, 2015, 122, 360-368.	1.6	20
214	Thermal and chemical stability of the β-W2N nitride phase. Nuclear Materials and Energy, 2017, 12, 462-467.	0.6	20
215	Thin films composed of metal nanoparticles (Au, Ag, Cu) dispersed in AlN: The influence of composition and thermal annealing on the structure and plasmonic response. Thin Solid Films, 2019, 676, 12-25.	0.8	20
216	Fuel inventory and material migration of JET main chamber plasma facing components compared over three operational periods. Physica Scripta, 2020, T171, 014051.	1.2	20

#	Article	IF	CITATIONS
217	Phase Transformation and Structural Studies of EUROFER RAFM Alloy. Materials Science Forum, 2006, 514-516, 500-504.	0.3	19
218	Comparison of ZnO thin films grown by pulsed laser deposition on sapphire and Si substrates. Physica E: Low-Dimensional Systems and Nanostructures, 2008, 40, 699-704.	1.3	19
219	Preparation and characterization of CrNxOy thin films: The effect of composition and structural features on the electrical behavior. Applied Surface Science, 2011, 257, 9120-9124.	3.1	19
220	Structural and optical properties of Ga auto-incorporated InAlN epilayers. Journal of Crystal Growth, 2014, 408, 97-101.	0.7	19
221	Luminescence studies on green emitting InGaN/GaN MQWs implanted with nitrogen. Scientific Reports, 2015, 5, 9703.	1.6	19
222	Photoluminescence studies of a perceived white light emission from a monolithic InGaN/GaN quantum well structure. Scientific Reports, 2015, 5, 13739.	1.6	19
223	Optical properties of zirconium oxynitride films: The effect of composition, electronic and crystalline structures. Applied Surface Science, 2015, 358, 660-669.	3.1	19
224	Evolution of the functional properties of titanium–silver thin films for biomedical applications: Influence of in-vacuum annealing. Surface and Coatings Technology, 2015, 261, 262-271.	2.2	19
225	Quantitative x-ray diffraction analysis of bimodal damage distributions in Tm implanted Al _{0.15} Ga _{0.85} N. Journal Physics D: Applied Physics, 2016, 49, 135308.	1.3	19
226	Thermal desorption spectrometry of beryllium plasma facing tiles exposed in the JET tokamak. Fusion Engineering and Design, 2018, 133, 135-141.	1.0	19
227	Engineering strain and conductivity of MoO3 by ion implantation. Acta Materialia, 2019, 169, 15-27.	3.8	19
228	Optical active centres in ZnO samples. Journal of Non-Crystalline Solids, 2006, 352, 1453-1456.	1.5	18
229	Failure mechanism of AlN nanocaps used to protect rare earth-implanted GaN during high temperature annealing. Applied Physics Letters, 2006, 88, 031902.	1.5	18
230	Effect of thermal treatments on the structure of MoNxOy thin films. Vacuum, 2008, 82, 1428-1432.	1.6	18
231	Adhesion failures on hard coatings induced by interface anomalies. Vacuum, 2009, 83, 1213-1217.	1.6	18
232	Low-temperature fabrication of layered self-organized Ge clusters by RF-sputtering. Nanoscale Research Letters, 2011, 6, 341.	3.1	18
233	The role and application of ion beam analysis for studies of plasma-facing components in controlled fusion devices. Nuclear Instruments & Methods in Physics Research B, 2016, 371, 4-11.	0.6	18
234	Behavior of liquid Li-Sn alloy as plasma facing material on ISTTOK. Fusion Engineering and Design, 2017, 117, 208-211.	1.0	18

#	Article	IF	CITATIONS
235	Characterization of magnetron sputtered sub-stoichiometric CrAlSiN x and CrAlSiO y N x coatings. Surface and Coatings Technology, 2017, 328, 134-141.	2.2	18
236	Analysis of deposited layers with deuterium and impurity elements on samples from the divertor of JET with ITER-like wall. Journal of Nuclear Materials, 2019, 516, 202-213.	1.3	18
237	W/AlSiTiNx/SiAlTiOyNx/SiAlOx multilayered solar thermal selective absorber coating. Solar Energy, 2020, 207, 192-198.	2.9	18
238	Hydrogenic retention of high-Z refractory metals exposed to ITER divertor-relevant plasma conditions. Nuclear Fusion, 2010, 50, 055004.	1.6	17
239	TiO ₂ coatings with Au nanoparticles analysed by photothermal IR radiometry. Journal Physics D: Applied Physics, 2012, 45, 105301.	1.3	17
240	Effects of helium and deuterium irradiation on SPS sintered W–Ta composites at different temperatures. Journal of Nuclear Materials, 2013, 442, S251-S255.	1.3	17
241	Europiumâ€doped GaN(Mg): beyond the limits of the lightâ€emitting diode. Physica Status Solidi C: Current Topics in Solid State Physics, 2014, 11, 662-665.	0.8	17
242	Study of damage formation and annealing of implanted III-nitride semiconductors for optoelectronic devices. Nuclear Instruments & Methods in Physics Research B, 2016, 379, 251-254.	0.6	17
243	Investigation and plasma cleaning of first mirrors coated with relevant ITER contaminants: beryllium and tungsten. Nuclear Fusion, 2017, 57, 086019.	1.6	17
244	WC-Cu thermal barriers for fusion applications. Surface and Coatings Technology, 2018, 355, 222-226.	2.2	17
245	Backscattering analysis of short period ZnO/MgO superlattices. Surface and Coatings Technology, 2018, 355, 45-49.	2.2	17
246	Deuterium retention and erosion in liquid Sn samples exposed to D2 and Ar plasmas in GyM device. Nuclear Materials and Energy, 2018, 17, 253-258.	0.6	17
247	RBS/C, XRR, and XRD Studies of Damage Buildup in Erâ€Implanted ZnO. Physica Status Solidi (B): Basic Research, 2019, 256, 1800364.	0.7	17
248	CrAlSiN barrier layer to improve the thermal stability of W/CrAlSiNx/CrAlSiOyNx/SiAlOx solar thermal absorber. Solar Energy Materials and Solar Cells, 2019, 191, 235-242.	3.0	17
249	Exchange bias of MnPt/CoFe films prepared by ion beam deposition. Journal of Applied Physics, 2004, 95, 6317-6321.	1.1	16
250	Annealing properties of ZnO films grown using diethyl zinc and tertiary butanol. Journal of Physics Condensed Matter, 2005, 17, 1719-1724.	0.7	16
251	Investigations of p-type signal for ZnO thin films grown on (100) GaAs substrates by pulsed laser deposition. Physica Status Solidi C: Current Topics in Solid State Physics, 2006, 3, 1038-1041.	0.8	16
252	TEM investigation of Tm implanted GaN, the influence of high temperature annealing. Optical Materials, 2006, 28, 738-741.	1.7	16

#	Article	IF	CITATIONS
253	Influence of air oxidation on the properties of decorative NbOxNy coatings prepared by reactive gas pulsing. Surface and Coatings Technology, 2008, 202, 2363-2367.	2.2	16
254	Functionalizing self-assembled GaN quantum dot superlattices by Eu-implantation. Journal of Applied Physics, 2010, 108, 084306.	1.1	16
255	Ageing effects on the wettability behavior of laser textured silicon. Applied Surface Science, 2011, 257, 2604-2609.	3.1	16
256	Electroless deposition of Au, Pt, or Ru metallic layers on CdZnTe. Thin Solid Films, 2012, 525, 56-63.	0.8	16
257	Rare earth co-doping nitride layers for visible light. Materials Chemistry and Physics, 2012, 134, 716-720.	2.0	16
258	Structural and optical studies of Au doped titanium oxide films. Nuclear Instruments & Methods in Physics Research B, 2012, 272, 61-65.	0.6	16
259	Extended-Gate ISFETs Based on Sputtered Amorphous Oxides. Journal of Display Technology, 2013, 9, 729-734.	1.3	16
260	Measurement of proton induced Î ³ -ray emission cross sections on Al from 2.5 to 4.1MeV. Nuclear Instruments & Methods in Physics Research B, 2014, 332, 355-358.	0.6	16
261	Raman study of insulating and conductive ZnO:(Al, Mn) thin films. Physica Status Solidi (A) Applications and Materials Science, 2015, 212, 2345-2354.	0.8	16
262	Metallic filamentary conduction in valence change-based resistive switching devices: the case of TaO _x thin film with <i>x</i> â^¼ 1. Nanoscale, 2019, 11, 16978-16990.	2.8	16
263	Amorphization of GaN by ion implantation. Nuclear Instruments & Methods in Physics Research B, 2001, 178, 200-203.	0.6	15
264	Depth profiling InGaN/GaN multiple quantum wells by Rutherford backscattering: The role of intermixing. Applied Physics Letters, 2002, 81, 2950-2952.	1.5	15
265	Influence of O and C co-implantation on the lattice site of Er in GaN. Applied Physics Letters, 2004, 84, 4304-4306.	1.5	15
266	Optical changes induced by high fluence implantation of Au ions on sapphire. Nuclear Instruments & Methods in Physics Research B, 2004, 218, 139-144.	0.6	15
267	Magnetic nanoscale aggregates of cobalt and nickel in MgO single crystals. European Physical Journal B, 2005, 45, 331-338.	0.6	15
268	Cathodoluminescence of rare earth implanted AlInN. Applied Physics Letters, 2006, 89, 131912.	1.5	15
269	Anisotropic ferromagnetism induced in rutile single crystals by Co implantation. European Physical Journal B, 2007, 55, 253-260.	0.6	15
270	Role of impurities and dislocations for the unintentional n-type conductivity in InN. Physica B: Condensed Matter, 2009, 404, 4476-4481.	1.3	15

#	Article	IF	CITATIONS
271	Influence of the AlN molar fraction on the structural and optical properties of praseodymium-doped AlxGa1⠰xN (0⩽x⩽1) alloys. Microelectronics Journal, 2009, 40, 377-380.	1.1	15
272	Erosion and re-deposition processes in JET tiles studied with ion beams. Nuclear Instruments & Methods in Physics Research B, 2010, 268, 1991-1996.	0.6	15
273	Deposition of13C tracer in the JET MkII-HD divertor. Physica Scripta, 2011, T145, 014004.	1.2	15
274	Enhanced dynamic annealing and optical activation of Eu implanted a-plane GaN. Europhysics Letters, 2012, 97, 68004.	0.7	15
275	Ion beam induced epitaxial crystallization of $\hat{I}\pm$ -Al2O3 at room temperature. Nuclear Instruments & Methods in Physics Research B, 2014, 321, 8-13.	0.6	15
276	Measuring strain caused by ion implantation in GaN. Materials Science in Semiconductor Processing, 2019, 98, 95-99.	1.9	15
277	An insider view of the Portuguese ion beam laboratory. European Physical Journal Plus, 2021, 136, 1.	1.2	15
278	Formation of coherent precipitates of platinum in sapphire. Nuclear Instruments & Methods in Physics Research B, 1999, 148, 1049-1053.	0.6	14
279	Effect of crystal orientation on defect production and optical activation of Er-implanted sapphire. Nuclear Instruments & Methods in Physics Research B, 2000, 166-167, 183-187.	0.6	14
280	Study of roughness in Ti0.4Al0.6N/Mo multilayer structures. Nuclear Instruments & Methods in Physics Research B, 2002, 188, 90-95.	0.6	14
281	PL studies on ZnO single crystals implanted with thulium ions. Superlattices and Microstructures, 2004, 36, 747-753.	1.4	14
282	Optical and structural studies in Eu-implanted AlN films. Superlattices and Microstructures, 2006, 40, 537-544.	1.4	14
283	Synthesis of ZnO nanocrystals in sapphire by ion implantation and vacuum annealing. Nuclear Instruments & Methods in Physics Research B, 2007, 257, 515-518.	0.6	14
284	Hydrogenic retention in tungsten exposed to ITER divertor relevant plasma flux densities. Journal of Nuclear Materials, 2009, 390-391, 610-613.	1.3	14
285	Compositional analysis and evolution of defects formed on GaInP epilayers grown on Germanium. Superlattices and Microstructures, 2009, 45, 277-284.	1.4	14
286	Consolidation of Cu-nDiamond Nanocomposites: Hot Extrusion vs Spark Plasma Sintering. Materials Science Forum, 2010, 636-637, 682-687.	0.3	14
287	Investigation of generation of defects due to metallization on CdZnTe detectors. Journal Physics D: Applied Physics, 2012, 45, 175102.	1.3	14
288	The effect of metalâ€rich growth conditions on the microstructure of Sc <i>_x</i> Ga _{1â^'<i>x</i>} N films grown using molecular beam epitaxy. Physica Status Solidi (A) Applications and Materials Science, 2015, 212, 2837-2842.	0.8	14

#	Article	IF	CITATIONS
289	Structure dependent resistivity and dielectric characteristics of tantalum oxynitride thin films produced by magnetron sputtering. Applied Surface Science, 2015, 354, 298-305.	3.1	14
290	Functional behaviour of TiO ₂ films doped with noble metals. Surface Engineering, 2016, 32, 554-561.	1.1	14
291	Deposition in the inner and outer corners of the JET divertor with carbon wall and metallic ITER-like wall. Physica Scripta, 2016, T167, 014052.	1.2	14
292	Raman microscopy investigation of beryllium materials. Physica Scripta, 2016, T167, 014027.	1.2	14
293	Up-conversion emission of aluminosilicate and titania films doped with Er3+/Yb3+ by ion implantation and sol-gel solution doping. Surface and Coatings Technology, 2018, 355, 162-168.	2.2	14
294	Ion irradiation-induced easy-cone anisotropy in double-MgO free layers for perpendicular magnetic tunnel junctions. Applied Physics Letters, 2018, 112, .	1.5	14
295	Eu-Doped AlGaN/GaN Superlattice-Based Diode Structure for Red Lighting: Excitation Mechanisms and Active Sites. ACS Applied Nano Materials, 2018, 1, 3845-3858.	2.4	14
296	Evaluation of tritium retention in plasma facing components during JET tritium operations. Physica Scripta, 2021, 96, 124075.	1.2	14
297	High temperature annealing of Er implanted GaN. Materials Science and Engineering B: Solid-State Materials for Advanced Technology, 2001, 81, 132-135.	1.7	13
298	Implantation and annealing studies of Tm-implanted GaN. Materials Science and Engineering B: Solid-State Materials for Advanced Technology, 2003, 105, 97-100.	1.7	13
299	High resolution backscattering studies of nanostructured magnetic and semiconducting materials. Nuclear Instruments & Methods in Physics Research B, 2005, 241, 454-458.	0.6	13
300	Structural and optical properties of Zn0.9Mn0.1O/ZnO core-shell nanowires designed by pulsed laser deposition. Journal of Applied Physics, 2009, 106, .	1.1	13
301	Strain dependence electrical resistance and cohesive strength of ITO thin films deposited on electroactive polymer. Thin Solid Films, 2010, 518, 4525-4528.	0.8	13
302	Raman study of dopedâ€ZnO thin films grown by rf sputtering. Physica Status Solidi C: Current Topics in Solid State Physics, 2010, 7, 2290-2293.	0.8	13
303	The high sensitivity of InN under rare earth ion implantation at medium range energy. Journal Physics D: Applied Physics, 2011, 44, 295402.	1.3	13
304	Incorporation of N in TiO2 films grown by DC-reactive magnetron sputtering. Nuclear Instruments & Methods in Physics Research B, 2012, 273, 109-112.	0.6	13
305	Composition and luminescence studies of InGaN epilayers grown at different hydrogen flow rates. Semiconductor Science and Technology, 2013, 28, 065011.	1.0	13
306	Development of tantalum oxynitride thin films produced by PVD: Study of structural stability. Applied Surface Science, 2013, 285, 19-26.	3.1	13

#	Article	IF	CITATIONS
307	Disorder induced violet/blue luminescence in rfâ€deposited ZnO films. Physica Status Solidi C: Current Topics in Solid State Physics, 2013, 10, 662-666.	0.8	13
308	Tribological characterization of TiO 2 /Au decorative thin films obtained by PVD magnetron sputtering technology. Wear, 2015, 330-331, 419-428.	1.5	13
309	Study of the electrical behavior of nanostructured Ti–Ag thin films, prepared by Glancing Angle Deposition. Materials Letters, 2015, 157, 188-192.	1.3	13
310	Spectroscopic Analysis of Eu ³⁺ Implanted and Annealed GaN Layers and Nanowires. Journal of Physical Chemistry C, 2015, 119, 17954-17964.	1.5	13
311	Thin films of Au-Al2O3 for plasmonic sensing. Applied Surface Science, 2020, 500, 144035.	3.1	13
312	Determination of non-Rutherford cross-sections from simple RBS spectra using Bayesian inference data analysis. Nuclear Instruments & Methods in Physics Research B, 2008, 266, 1180-1184.	0.6	12
313	Characterisation of titanium beryllides with different microstructure. Fusion Engineering and Design, 2009, 84, 1136-1139.	1.0	12
314	Microstructural characterization of the ODS Eurofer 97 EU-batch. Fusion Engineering and Design, 2011, 86, 2386-2389.	1.0	12
315	Microprobe analysis, iono- and photo-luminescence of Mn2+ activated ZnGa2O4 fibres. Nuclear Instruments & Methods in Physics Research B, 2013, 306, 195-200.	0.6	12
316	Doping of Ga ₂ O ₃ bulk crystals and NWs by ion implantation. Proceedings of SPIE, 2014, , .	0.8	12
317	Corundum-to-spinel structural phase transformation in alumina. Nuclear Instruments & Methods in Physics Research B, 2015, 358, 136-141.	0.6	12
318	Electrochemical characterization of nanostructured Ag:TiN thin films produced by glancing angle deposition on polyurethane substrates for bio-electrode applications. Journal of Electroanalytical Chemistry, 2016, 768, 110-120.	1.9	12
319	New WC-Cu thermal barriers for fusion applications: High temperature mechanical behaviour. Journal of Nuclear Materials, 2018, 498, 355-361.	1.3	12
320	New WC-Cu composites for the divertor in fusion reactors. Journal of Nuclear Materials, 2019, 521, 31-37.	1.3	12
321	Incorporation of Europium into GaN Nanowires by Ion Implantation. Journal of Physical Chemistry C, 2019, 123, 11874-11887.	1.5	12
322	Effect of composition and surface characteristics on fuel retention in beryllium-containing co-deposited layers. Physica Scripta, 2020, T171, 014038.	1.2	12
323	Effect of AlN content on the lattice site location of terbium ions in Al _{<i>x</i>} Ga _{1â^'<i>x</i>} N compounds. Semiconductor Science and Technology, 2016, 31, 035026.	1.0	12
324	Structural properties of CdTe and Hg1 â^' xCdxTe epitaxial layers grown on sapphire substrates. Journal of Crystal Growth, 1996, 161, 195-200.	0.7	11

#	Article	IF	CITATIONS
325	Laser-assisted recrystallization to improve the surface morphology of CdTe epitaxial layers. Semiconductor Science and Technology, 1996, 11, 248-251.	1.0	11
326	Anisotropic transport properties of epitaxial La2/3Ca1/3MnO3 thin films with different growth orientations (invited). Journal of Magnetism and Magnetic Materials, 2000, 211, 1-8.	1.0	11
327	Structural and optical characterization of topaz implanted with Fe and Co. Nuclear Instruments & Methods in Physics Research B, 2002, 191, 312-316.	0.6	11
328	Magnetic behavior of Co and Ni implanted MgO. Journal of Magnetism and Magnetic Materials, 2004, 272-276, 840-842.	1.0	11
329	Investigation of the nonlinear optical characteristics of composite materials based on sapphire with silver, copper, and gold nanoparticles by the reflection Z-scan method. Optics and Spectroscopy (English Translation of Optika I Spektroskopiya), 2006, 101, 615-622.	0.2	11
330	Influence of defects on the optical and structural properties of Ge dots embedded in an Si/Ge superlattice. Journal of Luminescence, 2006, 121, 417-420.	1.5	11
331	Diffusion processes in seeded and unseeded SBT thin films with varied stoichiometry. Surface Science, 2006, 600, 1780-1786.	0.8	11
332	Influence of Rapid Thermal Annealing on the Luminescence Properties of Nanoporous GaN Films. Electrochemical and Solid-State Letters, 2006, 9, G150.	2.2	11
333	Holistic RBS–PIXE data reanalysis of SBT thin film samples. Nuclear Instruments & Methods in Physics Research B, 2007, 261, 439-442.	0.6	11
334	Memory effect on CdSe nanocrystals embedded in SiO2 matrix. Solid State Communications, 2008, 148, 105-108.	0.9	11
335	Charging effects in CdSe nanocrystals embedded in SiO2 matrix produced by rf magnetron sputtering. Microelectronic Engineering, 2008, 85, 2374-2377.	1.1	11
336	Structural and optical properties of nitrogen doped ZnO films. Vacuum, 2009, 83, 1274-1278.	1.6	11
337	N-Doped Photocatalytic Titania Thin Films on Active Polymer Substrates. Journal of Nanoscience and Nanotechnology, 2010, 10, 1072-1077.	0.9	11
338	Mn-doped ZnO nanocrystals embedded in Al ₂ O ₃ : structural and electrical properties. Nanotechnology, 2010, 21, 505705.	1.3	11
339	Structural and optical properties of Er implanted AlN thin films: Green and infrared photoluminescence at room temperature. Optical Materials, 2011, 33, 1055-1058.	1.7	11
340	On the formation of an interface amorphous layer in nanostructured ferroelectric Ba0.8Sr0.2TiO3 thin films integrated on Pt–Si and its effect on the electrical properties. Applied Surface Science, 2013, 278, 136-141.	3.1	11
341	Formation and delamination of beryllium carbide films. Journal of Nuclear Materials, 2013, 442, S320-S324.	1.3	11
342	Influence of composition, bonding characteristics and microstructure on the electrochemical and optical stability of AlOxNy thin films. Electrochimica Acta, 2013, 106, 23-34.	2.6	11

#	Article	IF	CITATIONS
343	Helium and deuterium irradiation effects in W-Ta composites produced by pulse plasma compaction. Journal of Nuclear Materials, 2017, 492, 105-112.	1.3	11
344	Deposition in the tungsten divertor during the 2011–2016 campaigns in JET with ITER-like wall. Physica Scripta, 2020, T171, 014044.	1.2	11
345	Lattice location of Er in GaAs and Al0.5Ga0.5As layers grown by MBE on (100) GaAs substrates. Nuclear Instruments & Methods in Physics Research B, 1993, 80-81, 180-183.	0.6	10
346	Chemical effects on the amorphization of sapphire. Nuclear Instruments & Methods in Physics Research B, 1998, 141, 353-357.	0.6	10
347	Effect of crystal orientation on damage accumulation and post-implantation annealing for iron implantation into sapphire. Nuclear Instruments & Methods in Physics Research B, 1999, 148, 730-734.	0.6	10
348	Strain relaxation and compositional analysis of InGaN/GaN layers by Rutherford backscattering. Nuclear Instruments & Methods in Physics Research B, 2002, 190, 560-564.	0.6	10
349	Structural and optical studies of Co and Ti implanted sapphire. Nuclear Instruments & Methods in Physics Research B, 2003, 207, 55-62.	0.6	10
350	Optical absorption of a Li-related impurity in ZnO. Physica B: Condensed Matter, 2003, 340-342, 225-229.	1.3	10
351	Atomic environment and interfacial structural order of TiAlN/Mo multilayers. Surface and Coatings Technology, 2004, 187, 393-398.	2.2	10
352	Blue cathodoluminescence from thulium implanted AlxGa1â^'xN and InxAl1â^'xN. Superlattices and Microstructures, 2006, 40, 445-451.	1.4	10
353	Ion synthesis and optical properties of gold nanoparticles in an Al2O3 matrix. Technical Physics, 2006, 51, 1474-1481.	0.2	10
354	Structural and optical characterisation of Eu implanted AlxGa1â^'xN. Nuclear Instruments & Methods in Physics Research B, 2007, 257, 307-310.	0.6	10
355	Structural and optical properties on thulium-doped LHPG-grown Ta2O5 fibres. Microelectronics Journal, 2009, 40, 309-312.	1.1	10
356	Stopping power of 11B in Si and TiO2 measured with a bulk sample method and Bayesian inference data analysis. Nuclear Instruments & Methods in Physics Research B, 2010, 268, 1768-1771.	0.6	10
357	Al1â^'xInxN/GaN bilayers: Structure, morphology, and optical properties. Physica Status Solidi (B): Basic Research, 2010, 247, 1740-1746.	0.7	10
358	Isotopic fingerprints of Pt-containing luminescence centers in highly enrichedS28i. Physical Review B, 2010, 81, .	1.1	10
359	Doped gallium oxide nanowires for photonics. Proceedings of SPIE, 2012, , .	0.8	10
360	Structural and electrical studies of ultrathin layers with Si0.7Ge0.3 nanocrystals confined in a SiGe/SiO2 superlattice. Journal of Applied Physics, 2012, 111, 104323.	1.1	10

#	Article	IF	CITATIONS
361	Impact of implantation geometry and fluence on structural properties of AlxGa1-xN implanted with thulium. Journal of Applied Physics, 2016, 120, .	1.1	10
362	Asymmetric ZnO/ZnMgO double quantum well structures grown on m-plane ZnO substrates by MBE. Journal of Luminescence, 2017, 186, 262-267.	1.5	10
363	Validity of Vegard's rule for Al1â^'xInxN (0.08  <  x  < aꀉaꀉ0.28) thin films g Physics D: Applied Physics, 2017, 50, 205107.	rown on C	GaN template:
364	Tritium distributions on W-coated divertor tiles used in the third JET ITER-like wall campaign. Nuclear Materials and Energy, 2019, 18, 258-261.	0.6	10
365	Post-mortem analysis of tungsten plasma facing components in tokamaks: Raman microscopy measurements on compact, porous oxide and nitride films and nanoparticles. Nuclear Fusion, 2020, 60, 086004.	1.6	10
366	Solubility and damage annealing of Er implanted single crystalline α-Al2O3. Nuclear Instruments & Methods in Physics Research B, 1998, 139, 313-317.	0.6	9
367	Radioactive Isotope Identifications of Au and Pt Photoluminescence Centres in Silicon. Physica Status Solidi (B): Basic Research, 1998, 210, 853-858.	0.7	9
368	Study of Fe+ implanted GaN. Nuclear Instruments & Methods in Physics Research B, 2001, 175-177, 241-245.	0.6	9
369	The influence ofin situphotoexcitation on a defect structure generation in ArÂimplanted GaAs(001) crystals revealed by high-resolution x-ray diffraction and Rutherford backscattering spectroscopy. Journal Physics D: Applied Physics, 2003, 36, A143-A147.	1.3	9
370	PAC Studies of Implanted 111Ag in Single-Crystalline ZnO. Hyperfine Interactions, 2004, 158, 395-400.	0.2	9
371	Recent Emission Channeling Studies in Wide Band Gap Semiconductors. Hyperfine Interactions, 2004, 159, 363-372.	0.2	9
372	Optical and RBS studies in Tm implanted ZnO samples. Physica Status Solidi C: Current Topics in Solid State Physics, 2004, 1, 254-256.	0.8	9
373	Extended X-ray absorption fine structure studies of thulium doped GaN epilayers. Superlattices and Microstructures, 2004, 36, 729-736.	1.4	9
374	Li ceramic pebbles chemical compatibility with Eurofer samples in fusion relevant conditions. Journal of Nuclear Materials, 2004, 329-333, 1295-1299.	1.3	9
375	Luminescence and structural properties of defects in ion implanted ZnO. Physica Status Solidi C: Current Topics in Solid State Physics, 2006, 3, 968-971.	0.8	9
376	Optical properties tailoring by high fluence implantation of Ag ions on sapphire. Nuclear Instruments & Methods in Physics Research B, 2006, 242, 104-108.	0.6	9
377	Optical and structural behaviour of Cu-implanted sapphire. Surface and Coatings Technology, 2007, 201, 8190-8196.	2.2	9
378	Microstructural studies and electrical properties of Mg-doped SrTiO3 thin films. Acta Materialia, 2007, 55, 4947-4954.	3.8	9

#	Article	IF	CITATIONS
379	A comparative structural investigation of GaN implanted with rare earth ions at room temperature and 500ŰC. Materials Science and Engineering B: Solid-State Materials for Advanced Technology, 2008, 146, 204-207.	1.7	9
380	Stopping Power of Different Ions in Si Measured with a Bulk Sample Method and Bayesian Inference Data Analysis. , 2009, , .		9
381	Ion beam processing of sapphire single crystals. Surface and Coatings Technology, 2009, 203, 2357-2362.	2.2	9
382	Morphological and optical properties of silicon thin films by PLD. Applied Surface Science, 2009, 255, 5299-5302.	3.1	9
383	Photosensitivity of nanocrystalline ZnO films grown by PLD. Applied Surface Science, 2009, 255, 5917-5921.	3.1	9
384	Structural study of Si1â^'xGex nanocrystals embedded in SiO2 films. Thin Solid Films, 2010, 518, 2569-2572.	0.8	9
385	Comparative study of fusion relevant properties of Be12V and Be12Ti. Fusion Engineering and Design, 2011, 86, 2454-2457.	1.0	9
386	Tritium permeation, retention and release properties of beryllium pebbles. Fusion Engineering and Design, 2011, 86, 2338-2342.	1.0	9
387	Free electron properties and hydrogen in InN grown by MOVPE. Physica Status Solidi (A) Applications and Materials Science, 2011, 208, 1179-1182.	0.8	9
388	Ternary AlGaN Alloys with High Al Content and Enhanced Compositional Homogeneity Grown by Plasma-Assisted Molecular Beam Epitaxy. Japanese Journal of Applied Physics, 2011, 50, 031001.	0.8	9
389	Structural and magnetic properties of thin films of BaFeO3-Î′ deposited by pulsed injection metal-organic chemical vapor deposition. Journal of Applied Physics, 2012, 111, .	1.1	9
390	Deposition of nanometric double layers Ru/Au, Ru/Pd, and Pd/Au onto CdZnTe by the electroless method. Journal of Crystal Growth, 2012, 358, 89-93.	0.7	9
391	The electronic transport mechanism in indium molybdenum oxide thin films RF sputtered at room temperature. Europhysics Letters, 2012, 97, 36002.	0.7	9
392	Ion implantation of Cd and Ag into AlN and GaN. Physica Status Solidi C: Current Topics in Solid State Physics, 2012, 9, 1060-1064.	0.8	9
393	Sequential multiple-step europium ion implantation and annealing of GaN. Physica Status Solidi C: Current Topics in Solid State Physics, 2014, 11, 253-257.	0.8	9
394	Analysis of rotating collectors from the private region of JET with carbon wall and metallic ITER-like wall. Journal of Nuclear Materials, 2015, 463, 818-821.	1.3	9
395	Electrochemical and structural characterization of nanocomposite Agy:TiNx thin films for dry bioelectrodes: the effect of the N/Ti ratio and Ag content. Electrochimica Acta, 2015, 153, 602-611.	2.6	9
396	Peculiar Magnetoelectric Coupling in BaTiO ₃ :Fe _{113Âppm} Nanoscopic Segregations. ACS Applied Materials & Interfaces, 2015, 7, 24741-24747.	4.0	9

#	Article	IF	CITATIONS
397	Spectroscopic analysis of the NIR emission in Tm implanted AlxGa1-xN layers. Journal of Applied Physics, 2016, 120, 081701.	1.1	9
398	Determination of 9Be(p,p0)9Be, 9Be(p,d0)8Be and 9Be(p,α0)6Li cross sections at 150° in the energy range 0.5–2.35 MeV. Nuclear Instruments & Methods in Physics Research B, 2016, 371, 50-53.	0.6	9
399	Defect formation and optical activation of Tb implanted AlxGa1â^'xN films using channeled implantation at different temperatures. Surface and Coatings Technology, 2018, 355, 29-39.	2.2	9
400	Optical investigations of europium ion implanted in nitride-based diode structures. Surface and Coatings Technology, 2018, 355, 40-44.	2.2	9
401	Crystal damage analysis of implanted AlxGa1-xN (0â€ ⁻ â‰≇€ ⁻ xâ€ ⁻ â‰≇€ ⁻ 1) by ion beam techniques. Surface and Technology, 2018, 355, 55-60.	Coatings 2.2	9
402	Deposition temperature influence on the wear behaviour of carbon-based coatings deposited on hardened steel. Applied Surface Science, 2019, 475, 762-773.	3.1	9
403	Lattice site location and annealing behavior of W implanted TiO2. Nuclear Instruments & Methods in Physics Research B, 1998, 136-138, 442-446.	0.6	8
404	Annealing behaviour of natural topaz implanted with W and Cr ions. Nuclear Instruments & Methods in Physics Research B, 2000, 166-167, 204-208.	0.6	8
405	Indium content determination related with structural and optical properties of InGaN layers. Journal of Crystal Growth, 2001, 230, 448-453.	0.7	8
406	Optical studies on the red luminescence of InGaN epilayers. Superlattices and Microstructures, 2004, 36, 625-632.	1.4	8
407	Depth profiling of ion-implanted AlInN using time-of-flight secondary ion mass spectrometry and cathodoluminescence. Physica Status Solidi C: Current Topics in Solid State Physics, 2006, 3, 1927-1930.	0.8	8
408	Behaviour of the AlN cap during GaN implantation of rare earths and annealing. Physica Status Solidi (A) Applications and Materials Science, 2006, 203, 2172-2175.	0.8	8
409	Compositional and structural changes in ZrOxNy films depending on growth condition. Nuclear Instruments & Methods in Physics Research B, 2006, 249, 458-461.	0.6	8
410	Optical properties of high-temperature annealed Eu-implanted GaN. Optical Materials, 2006, 28, 797-801.	1.7	8
411	Structural and optical properties of Er3+ion in sol–gel grown LiNbO3. Journal of Physics Condensed Matter, 2007, 19, 016213.	0.7	8
412	Mechanisms of AlInN growth by MOVPE: modeling and experimental study. Physica Status Solidi C: Current Topics in Solid State Physics, 2008, 5, 1688-1690.	0.8	8
413	Rare earth doping of Illâ€nitride alloys by ion implantation. Physica Status Solidi (A) Applications and Materials Science, 2008, 205, 34-37.	0.8	8
414	Europium doping of zincblende GaN by ion implantation. Journal of Applied Physics, 2009, 105, 113507.	1.1	8

#	Article	IF	CITATIONS
415	Multilayers of Ge nanocrystals embedded in Al2O3 matrix: Structural and electrical studies. Microelectronic Engineering, 2010, 87, 2508-2512.	1.1	8
416	Electrical and Raman Scattering Studies of ZnO:P and ZnO:Sb Thin Films. Journal of Nanoscience and Nanotechnology, 2010, 10, 2620-2623.	0.9	8
417	Influence of the deposition parameters on the growth of SiGe nanocrystals embedded in Al2O3 matrix. Microelectronic Engineering, 2011, 88, 509-513.	1.1	8
418	Surface Plasmon Resonance Effect on the Optical Properties of TiO ₂ Doped by Noble Metals Nanoparticles. Journal of Nano Research, 0, 18-19, 177-185.	0.8	8
419	Influence of annealing conditions on the formation of regular lattices of voids and Ge quantum dots in an amorphous alumina matrix. Nanotechnology, 2012, 23, 405605.	1.3	8
420	Stopping power of He, C and O in TiO2. Nuclear Instruments & Methods in Physics Research B, 2012, 273, 22-25.	0.6	8
421	High precision determination of the InN content of Al1â^'xInxN thin films by Rutherford backscattering spectrometry. Nuclear Instruments & Methods in Physics Research B, 2012, 273, 105-108.	0.6	8
422	A comparative study of photo-, cathodo- and ionoluminescence of GaN nanowires implanted with rare earth ions. Nuclear Instruments & Methods in Physics Research B, 2013, 306, 201-206.	0.6	8
423	Towards the understanding of the intentionally induced yellow luminescence in GaN nanowires. Physica Status Solidi C: Current Topics in Solid State Physics, 2013, 10, 667-672.	0.8	8
424	Helium load on W-O coatings grown by pulsed laser deposition. Surface and Coatings Technology, 2018, 355, 215-221.	2.2	8
425	Radiation sensors based on GaN microwires. Journal Physics D: Applied Physics, 2018, 51, 175105.	1.3	8
426	Multiple optical centers in Eu-implanted AlN nanowires for solid-state lighting applications. Applied Physics Letters, 2018, 113, 201905.	1.5	8
427	CuxCrFeMoTi (x = 0.21, 0.44, 1) high entropy alloys as novel materials for fusion applications. Materials Science and Engineering B: Solid-State Materials for Advanced Technology, 2018, 238-239, 18-25.	1.7	8
428	Measurement of proton induced γ-ray emission cross sections on Na from 1.0 to 4.1 MeV. Nuclear Instruments & Methods in Physics Research B, 2019, 441, 108-118.	0.6	8
429	Stopping power of hydrogen in hafnium and the importance of relativistic <mml:math xmlns:mml="http://www.w3.org/1998/Math/MathML"> <mml:mrow> <mml:mn>4</mml:mn> <mml:mi> electrons. Physical Review A, 2020, 101, .</mml:mi></mml:mrow></mml:math 	< ‡ro ml:mr	:08/>
430	Study of structural and optical properties of MBE grown nonpolar (10-10) ZnO/ZnMgO photonic structures. Optical Materials, 2020, 100, 109709.	1.7	8
431	Nanocomposite Au-ZnO thin films: Influence of gold concentration and thermal annealing on the microstructure and plasmonic response. Surface and Coatings Technology, 2020, 385, 125379.	2.2	8
432	Crystal mosaicity determined by a novel layer deconvolution Williamson–Hall method. CrystEngComm, 2021, 23, 2048-2062.	1.3	8

#	Article	IF	CITATIONS
433	In-situ annealing transmission electron microscopy of plasmonic thin films composed of bimetallic Au–Ag nanoparticles dispersed in a TiO2 matrix. Vacuum, 2021, 193, 110511.	1.6	8
434	Enhancing the luminescence yield of Cr3+ in <i>β</i> -Ga2O3 by proton irradiation. Applied Physics Letters, 2022, 120, .	1.5	8
435	Selective area vapor-phase epitaxy and structural properties of Hg1 â^' xCdxTe on sapphire. Journal of Crystal Growth, 1997, 179, 585-591.	0.7	7
436	Influence of oxygen ion implantation on the damage and annealing kinetics of iron-implanted sapphire. Nuclear Instruments & Methods in Physics Research B, 2000, 166-167, 188-192.	0.6	7
437	Depth Resolved Studies of Indium Content and Strain in InGaN Layers. Physica Status Solidi (B): Basic Research, 2001, 228, 59-64.	0.7	7
438	Study of new surface structures created on sapphire by Co ion implantation. Nuclear Instruments & Methods in Physics Research B, 2001, 175-177, 500-504.	0.6	7
439	Effects of ion implantation on the thermoluminescent properties of natural colourless topaz. Nuclear Instruments & Methods in Physics Research B, 2002, 191, 196-201.	0.6	7
440	Influence of annealing atmosphere on the behavior of titanium implanted sapphire. Nuclear Instruments & Methods in Physics Research B, 2002, 191, 644-648.	0.6	7
441	Interrelation between microstructure and optical properties of erbium-doped nanocrystalline thin films. Physica E: Low-Dimensional Systems and Nanostructures, 2003, 16, 414-419.	1.3	7
442	Analysis of Strain Depth Variations in an In0.19Ga0.81N Layer by Raman Spectroscopy. Physica Status Solidi C: Current Topics in Solid State Physics, 2003, 0, 563-567.	0.8	7
443	Optical and mechanical properties of MgO crystals implanted with lithium ions. Journal of Applied Physics, 2004, 95, 2371-2378.	1.1	7
444	Copper nanocolloids in MgO crystals implanted with Cu ions. Nuclear Instruments & Methods in Physics Research B, 2004, 218, 148-152.	0.6	7
445	Compositional Profiles in Silica-Based Sol-Gel Films Doped with Erbium and Silver, by RBS and ERDA. Journal of Sol-Gel Science and Technology, 2004, 31, 287-291.	1.1	7
446	Copper and cobalt nanocolloids in implanted MgO crystals. Nuclear Instruments & Methods in Physics Research B, 2007, 257, 563-567.	0.6	7
447	Radiation hardness of GeSi heterostructures with thin Ge layers. Materials Science and Engineering B: Solid-State Materials for Advanced Technology, 2008, 147, 191-194.	1.7	7
448	Evaluation of exposure parameters in plain radiography: a comparative study with European guidelines. Radiation Protection Dosimetry, 2008, 129, 316-320.	0.4	7
449	Co-doping of aluminium and gallium with nitrogen in ZnO films deposited by RF magnetron sputtering. Journal of Physics Condensed Matter, 2008, 20, 075220.	0.7	7
450	Intrinsic <i>p</i> Type ZnO Films Deposited by rf Magnetron Sputtering. Journal of Nanoscience and Nanotechnology, 2009, 9, 813-816.	0.9	7

#	Article	IF	CITATIONS
451	Microstructural evolution in tungsten and copper probes under hydrogen irradiation at ISTTOK. Journal of Nuclear Materials, 2009, 390-391, 1039-1042.	1.3	7
452	Electrical properties of sol–gel derived MPB 0.37BiScO3–0.63PbTiO3 thin films deposited on iridium oxide electrodes. Journal of Materials Chemistry, 2009, 19, 5572.	6.7	7
453	Effect of Eu2O3 doping on Ta2O5 crystal growth by the laser-heated pedestal technique. Journal of Crystal Growth, 2010, 313, 62-67.	0.7	7
454	Room temperature paramagnetism of ZnO:Mn films grown by RF-sputtering. Thin Solid Films, 2010, 518, 4612-4614.	0.8	7
455	The Characterization of N Interstitials and Dangling Bond Point Defects on Ionâ€Implanted GaN Nanowires Studied by Photoluminescence and Xâ€Ray Absorption Spectroscopy. Journal of the American Ceramic Society, 2010, 93, 3531-3534.	1.9	7
456	Microstructure and nanomechanical properties of Fe+ implanted silicon. Applied Surface Science, 2013, 284, 533-539.	3.1	7
457	Formation of oriented nickel aggregates in rutile single crystals by Ni implantation. Journal of Magnetism and Magnetic Materials, 2013, 340, 102-108.	1.0	7
458	Composition, structure and morphology of Al _{1â^'<i>x</i>} In _{<i>x</i>} N thin films grown on Al _{1â^'<i>y</i>} Ga _{<i>y</i>} N templates with different GaN contents. Journal Physics D: Applied Physics, 2015, 48, 015103.	1.3	7
459	Composition and structure variation for magnetron sputtered tantalum oxynitride thin films, as function of deposition parameters. Applied Surface Science, 2015, 358, 508-517.	3.1	7
460	Electrical insulation properties of RF-sputtered LiPON layers towards electrochemical stability of lithium batteries. Journal Physics D: Applied Physics, 2016, 49, 485301.	1.3	7
461	Analysis of the Tb3+ recombination in ion implanted Al Ga1â^'N (O≤â‰⊉) layers. Journal of Luminescence, 2016, 178, 249-258.	1.5	7
462	Study of deuterium retention in Be-W coatings with distinct roughness profiles. Fusion Engineering and Design, 2017, 124, 464-467.	1.0	7
463	In Situ Characterization and Modification of βâ€Ga ₂ O ₃ Flakes Using an Ion Microâ€Probe. Physica Status Solidi (A) Applications and Materials Science, 2018, 215, 1800190.	0.8	7
464	The effect of increasing Si content in the absorber layers (CrAlSiNx/CrAlSiOyNx) of solar selective absorbers upon their selectivity and thermal stability. Applied Surface Science, 2019, 481, 1096-1102.	3.1	7
465	Improved neutron activation dosimetry for fusion. Fusion Engineering and Design, 2019, 139, 109-114.	1.0	7
466	Dependence of optical properties on composition of silicon carbonitride thin films deposited at low temperature by PECVD. Journal of Non-Crystalline Solids, 2021, 551, 120434.	1.5	7
467	RE Implantation and Annealing of III-Nitrides. Topics in Applied Physics, 2010, , 25-54.	0.4	7
468	Fuel retention and erosion-deposition on inner wall cladding tiles in JET-ILW. Physica Scripta, 2021, 96, 124071.	1.2	7

#	Article	IF	CITATIONS
469	Vacancy-acceptor complexes in germanium produced by ion implantation. Nuclear Instruments & Methods in Physics Research B, 1991, 59-60, 1049-1052.	0.6	6
470	Structural properties of layers grown on CdTe substrates by liquid phase epitaxy. Semiconductor Science and Technology, 1996, 11, 542-547.	1.0	6
471	Ion beam studies of CdTe films epitaxially grown on Si, GaAs and sapphire substrates. Nuclear Instruments & Methods in Physics Research B, 1998, 136-138, 220-224.	0.6	6
472	Properties of epitaxial LaCaMnO laser ablated thin films on (1 0 0) and (1 1 0) SrTiO3 substrates. Journal of Magnetism and Magnetic Materials, 1999, 196-197, 495-497.	1.0	6
473	Influence of Temperature and Pressure on the Beryllium Pebbles Bed Electrical Resistivity. Fusion Science and Technology, 2000, 38, 320-325.	0.6	6
474	Surface studies of SiC/SiCf composites exposed to relevant fusion reactor conditions. Surface and Interface Analysis, 2000, 30, 98-100.	0.8	6
475	Luminescence studies in colour centres produced in natural topaz. Journal of Luminescence, 2000, 87-89, 583-585.	1.5	6
476	Preliminary investigations of infrared Er-related photoluminescence in ion-implanted In0.07Ga0.93N. Applied Physics Letters, 2002, 80, 4504-4506.	1.5	6
477	Ion beam studies of MBE grown GaN films on silicon substrates. Nuclear Instruments & Methods in Physics Research B, 2002, 188, 73-77.	0.6	6
478	Analysis of sapphire implanted with different elements using artificial neural networks. Nuclear Instruments & Methods in Physics Research B, 2002, 190, 241-246.	0.6	6
479	The structure of sapphire implanted with nitrogen at room temperature and 1000 °C. Nuclear Instruments & Methods in Physics Research B, 2002, 191, 629-632.	0.6	6
480	Radiation-damage recovery in undoped and oxidized Li doped MgO crystals implanted with lithium ions. Nuclear Instruments & Methods in Physics Research B, 2003, 206, 148-152.	0.6	6
481	High Temperature Implantation of Tm in GaN. Materials Research Society Symposia Proceedings, 2003, 798, 548.	0.1	6
482	Defect production in nitrogen implanted sapphire. Nuclear Instruments & Methods in Physics Research B, 2004, 218, 222-226.	0.6	6
483	Electrical conductivity of as-grown and oxidized MgO:Li crystals implanted with Li ions. Nuclear Instruments & Methods in Physics Research B, 2004, 218, 164-169.	0.6	6
484	Characterisation of defects in rare earth implanted GaN by deep level transient spectroscopy. Superlattices and Microstructures, 2004, 36, 713-719.	1.4	6
485	Optical and structural study of Ge/Si quantum dots on Si(100) surface covered with a thin silicon oxide layer. Materials Science and Engineering B: Solid-State Materials for Advanced Technology, 2005, 124-125, 462-465.	1.7	6
486	Ion beam analysis of GaInAsSb films grown by MOVPE on GaSb. Nuclear Instruments & Methods in Physics Research B, 2005, 241, 326-330.	0.6	6

#	Article	IF	CITATIONS
487	Radiation-induced defects in a-Si:H by 1.5MeV He4 particles studied by photoconductivity and photothermal deflection spectroscopy. Journal of Non-Crystalline Solids, 2006, 352, 1071-1074.	1.5	6
488	Ion beam characterisation of ODS steel samples after long term annealing conditions. Nuclear Instruments & Methods in Physics Research B, 2006, 249, 493-496.	0.6	6
489	Lattice order in thulium-doped GaN epilayers: In situ doping versus ion implantation. Optical Materials, 2006, 28, 771-774.	1.7	6
490	Optical activation of Eu ions in nanoporous GaN films. Journal of Applied Physics, 2006, 99, 104305.	1.1	6
491	Relaxation behaviour of Co and Ni implanted into MgO. Journal of Magnetism and Magnetic Materials, 2007, 316, e776-e778.	1.0	6
492	Elemental and RBS analysis of hybrid materials prepared by gamma-irradiation. Nuclear Instruments & Methods in Physics Research B, 2008, 266, 288-294.	0.6	6
493	Electrical conductivity in undoped α-Al2O3 crystals implanted with Mg ions. Nuclear Instruments & Methods in Physics Research B, 2008, 266, 2932-2935.	0.6	6
494	Microwave dielectric permittivity and photoluminescence of Eu2O3 doped laser heated pedestal growth Ta2O5 fibers. Applied Physics Letters, 2008, 92, 252904.	1.5	6
495	Two colour experiments in Eu3+ implanted GaN. Journal of Alloys and Compounds, 2008, 451, 140-142.	2.8	6
496	Influence of steering effects on strain detection in AlGaInN/GaN heterostructures by ion channelling. Journal Physics D: Applied Physics, 2009, 42, 065420.	1.3	6
497	Comparison of the damage in sapphire due to implantation of boron, nitrogen, and iron. Journal of Nuclear Materials, 2009, 389, 311-316.	1.3	6
498	Effect of annealing on AlN/GaN quantum dot heterostructures: advanced ion beam characterization and Xâ€ray study of lowâ€dimensional structures. Surface and Interface Analysis, 2010, 42, 1552-1555.	0.8	6
499	Surface composition and morphology changes of JET tiles under plasma interactions. Fusion Engineering and Design, 2011, 86, 2557-2560.	1.0	6
500	Tungsten–microdiamond composites for plasma facing components. Journal of Nuclear Materials, 2011, 416, 45-48.	1.3	6
501	Effect of Eu-implantation and annealing on the GaN quantum dots excitonic recombination. Nanoscale Research Letters, 2011, 6, 378.	3.1	6
502	Zeeman splittings of the ⁵ D ₀ – ⁷ F ₂ transitions of Eu ³⁺ ions implanted into GaN. Materials Research Society Symposia Proceedings, 2011, 1290, 1.	0.1	6
503	Cd ion implantation in AlN. Nuclear Instruments & Methods in Physics Research B, 2012, 289, 43-46.	0.6	6
504	Lattice site location and luminescence studies of AlxGa1â^'xN alloys doped with thulium ions. Nuclear Instruments & Methods in Physics Research B, 2013, 307, 495-498.	0.6	6

#	Article	IF	CITATIONS
505	Thermal properties of holmium-implanted gold films for a neutrino mass experiment with cryogenic microcalorimeters. Review of Scientific Instruments, 2013, 84, 083905.	0.6	6
506	Analysis of the stability of InGaN/GaN multiquantum wells against ion beam intermixing. Nanotechnology, 2015, 26, 425703.	1.3	6
507	Optical performance of thin films produced by the pulsed laser deposition of SiAlON and Er targets. Applied Surface Science, 2015, 336, 274-277.	3.1	6
508	Magnetoelectric effect probe through ppm Fe doping in BaTiO 3. Journal of Alloys and Compounds, 2016, 661, 495-500.	2.8	6
509	Study of In distribution on GaInSb:Al crystals by ion beam techniques. Nuclear Instruments & Methods in Physics Research B, 2016, 371, 278-282.	0.6	6
510	Effects of thermal annealing on the structural and electronic properties of rare earth-implanted MoO ₃ nanoplates. CrystEngComm, 2017, 19, 2339-2348.	1.3	6
511	Impurity re-distribution in the corner regions of the JET divertor. Physica Scripta, 2017, T170, 014060.	1.2	6
512	Ar ⁺ ion irradiation of magnetic tunnel junction multilayers: impact on the magnetic and electrical properties. Journal Physics D: Applied Physics, 2020, 53, 455003.	1.3	6
513	Multiple reflection optimization package for X-ray diffraction. CrystEngComm, 2021, 23, 3308-3318.	1.3	6
514	Simulating the effect of Ar+ energy implantation on the strain propagation in AlGaN. Journal Physics D: Applied Physics, 2021, 54, 245301.	1.3	6
515	Lattice Location Studies on Hafnium, Thallium and Lead Implanted Magnesium Single Crystals. , 1984, , 74-82.		6
516	Time-resolved deposition in the remote region of the JET-ILW divertor: measurements and modelling. Physica Scripta, 2017, T170, 014059.	1.2	6
517	Ta2O5/SiO2 Multicomponent Dielectrics for Amorphous Oxide TFTs. Electronic Materials, 2021, 2, 1-16.	0.9	6
518	Tantalum-Titanium Oxynitride Thin Films Deposited by DC Reactive Magnetron Co-Sputtering: Mechanical, Optical, and Electrical Characterization. Coatings, 2022, 12, 36.	1.2	6
519	Epitaxial regrowth and lattice location of indium implanted in arsenic-preamorphized silicon. Nuclear Instruments & Methods in Physics Research B, 1991, 55, 580-584.	0.6	5
520	Hyperfine fields of mercury in singleâ€crystalline cobalt. Journal of Applied Physics, 1994, 76, 6906-6908.	1.1	5
521	Ion beam mixing of chromium or zirconium films with sapphire. Surface and Coatings Technology, 1996, 83, 151-155.	2.2	5
522	The Photoluminescence of Pt-Implanted Silicon. Materials Science Forum, 1997, 258-263, 473-478.	0.3	5

#	Article	IF	CITATIONS
523	Lattice site location of thulium and erbium implanted GaAs. Nuclear Instruments & Methods in Physics Research B, 1998, 136-138, 421-425.	0.6	5
524	Molecular H2 and H3 energy loss measurements along the Si ã€^111〉 direction. Nuclear Instruments & Methods in Physics Research B, 2000, 161-163, 168-171.	0.6	5
525	Green and red emission in Ca implanted GaN samples. Physica B: Condensed Matter, 2001, 308-310, 42-46.	1.3	5
526	Artificial neural network analysis of RBS data of Er-implanted sapphire. Nuclear Instruments & Methods in Physics Research B, 2001, 175-177, 108-112.	0.6	5
527	Cadmium addition to vacancy doped lanthanum manganites: from metallic to insulator behaviour. Journal of Magnetism and Magnetic Materials, 2001, 226-230, 797-799.	1.0	5
528	Optical activity and damage recovery of erbium implanted strontium titanate. Radiation Effects and Defects in Solids, 2002, 157, 1071-1076.	0.4	5
529	Study of calcium implanted GaN. Nuclear Instruments & Methods in Physics Research B, 2002, 190, 625-629.	0.6	5
530	Nanoindentation on MgO crystals implanted with lithium ions. Nuclear Instruments & Methods in Physics Research B, 2002, 191, 154-157.	0.6	5
531	Erbium implantation in strontium titanate. Nuclear Instruments & Methods in Physics Research B, 2002, 191, 317-322.	0.6	5
532	Optical changes induced by high fluence implantation of Co ions on sapphire. Surface and Coatings Technology, 2002, 158-159, 54-58.	2.2	5
533	Processing of rare earth doped GaN with ion beams. Materials Research Society Symposia Proceedings, 2003, 798, 569.	0.1	5
534	The effect of temperature on the structure of iron-implanted sapphire. Nuclear Instruments & Methods in Physics Research B, 2004, 218, 227-231.	0.6	5
535	Study of silica–titania films doped with Er and Ag by RBS and ERDA. Nuclear Instruments & Methods in Physics Research B, 2004, 219-220, 923-927.	0.6	5
536	The atomic structure of defects formed during doping of GaN with rare earth ions. Physica Status Solidi C: Current Topics in Solid State Physics, 2005, 2, 1081-1084.	0.8	5
537	RBS/channeling study of buried Ge quantum dots grown in a Si layer. Nuclear Instruments & Methods in Physics Research B, 2006, 249, 462-465.	0.6	5
538	Combination of IBA Techniques for Composition Analysis of GalnAsSb Films. Materials Science Forum, 2006, 514-516, 1603-1607.	0.3	5
539	Temperature dependence of the electric field gradient in GaN measured with the PAC-probe 181Hf. Hyperfine Interactions, 2007, 177, 89-95.	0.2	5
540	Breakdown of anomalous channeling with ion energy for accurate strain determination in GaN-based heterostructures. Applied Physics Letters, 2009, 95, 051921.	1.5	5

Eduardo Alves

#	Article	IF	CITATIONS
541	Phase transitions in erbium-doped silicon exposed to laser radiation. Journal of Applied Spectroscopy, 2009, 76, 209-214.	0.3	5
542	New Approaches to Thermoelectric Materials. NATO Science for Peace and Security Series B: Physics and Biophysics, 2009, , 51-67.	0.2	5
543	Crystal Size and Crystalline Volume Fraction Effects on the Erbium Emission of nc-Si:Er Grown by r.f. Sputtering. Journal of Nanoscience and Nanotechnology, 2010, 10, 2663-2668.	0.9	5
544	Effect of grain size and hydrogen passivation on the electrical properties of nanocrystalline silicon films. International Journal of Materials and Product Technology, 2010, 39, 195.	0.1	5
545	Damage recovery and optical activity in europium implanted wide gap oxides. Nuclear Instruments & Methods in Physics Research B, 2010, 268, 3137-3141.	0.6	5
546	Influence of thermal annealing on the structural and optical properties of GaN/AlN quantum dots. Physica Status Solidi (B): Basic Research, 2010, 247, 1675-1678.	0.7	5
547	Optical doping of Al[sub x]Ga[sub 1â^'x]N compounds by ion implantation of Tm ions. AIP Conference Proceedings, 2012, , .	0.3	5
548	Stopping power of C in Si. Nuclear Instruments & Methods in Physics Research B, 2012, 273, 30-32.	0.6	5
549	Measurement and evaluation of the 13C(p,p)13C cross section in the energy range 0.8–2.4MeV. Nuclear Instruments & Methods in Physics Research B, 2013, 316, 81-87.	0.6	5
550	Temperature-dependent hysteresis of the emission spectrum of Eu-implanted, Mg-doped HVPE GaN. AIP Conference Proceedings, 2013, , .	0.3	5
551	GaN:Pr ³⁺ nanostructures for red solid state light emission. RSC Advances, 2014, 4, 62869-62877.	1.7	5
552	Stopping power of C, O and Cl in tantalum oxide. Nuclear Instruments & Methods in Physics Research B, 2014, 332, 152-155.	0.6	5
553	Performance of resistive-charge position sensitive detectors for RBS/Channeling applications. Nuclear Instruments and Methods in Physics Research, Section A: Accelerators, Spectrometers, Detectors and Associated Equipment, 2014, 760, 98-106.	0.7	5
554	Correction to "Spectroscopic Analysis of Eu ³⁺ Implanted and Annealed GaN Layers and Nanowires― Journal of Physical Chemistry C, 2016, 120, 6907-6908.	1.5	5
555	SiGe layer thickness effect on the structural and optical properties of well-organized SiGe/SiO2multilayers. Nanotechnology, 2017, 28, 345701.	1.3	5
556	Electrical characterization of molybdenum oxide lamellar crystals irradiated with UV light and proton beams. Surface and Coatings Technology, 2018, 355, 50-54.	2.2	5
557	Deuterium retention on the tungsten-coated divertor tiles of JET ITER-like wall in 2015–2016 campaign. Fusion Engineering and Design, 2019, 146, 1979-1982.	1.0	5
558	Optical and photoconductive properties of indium sulfide fluoride thin films. Thin Solid Films, 2019, 671, 49-52.	0.8	5

#	Article	IF	CITATIONS
559	A study of solar thermal absorber stack based on CrAlSiNx/CrAlSiNxOy structure by ion beams. Nuclear Instruments & Methods in Physics Research B, 2019, 450, 195-199.	0.6	5
560	Microwave transient reflection in annealed SnS thin films. Materials Science in Semiconductor Processing, 2021, 121, 105302.	1.9	5
561	The effects of mechanical alloying on the physical and thermal properties of CuCrFeTiV alloy. Materials Science and Engineering B: Solid-State Materials for Advanced Technology, 2021, 263, 114805.	1.7	5
562	Me-Doped Ti–Me Intermetallic Thin Films Used for Dry Biopotential Electrodes: A Comparative Case Study. Sensors, 2021, 21, 8143.	2.1	5
563	Lattice Location and Photoluminescence of Er in GaAs and Al0.5Ga0.5As. Materials Research Society Symposia Proceedings, 1993, 301, 175.	0.1	4
564	The substitutionality of hafnium in sapphire by ion implantation and low temperature annealing. Nuclear Instruments & Methods in Physics Research B, 1995, 106, 602-605.	0.6	4
565	Microscopic studies of radioactive Hg implanted in YBa 2Cu3O6 + x superconducting thin films. Journal of Magnetism and Magnetic Materials, 1998, 177-181, 511-512.	1.0	4
566	Lattice location and annealing behaviour of Pt and W implanted sapphire. Nuclear Instruments & Methods in Physics Research B, 1999, 147, 226-230.	0.6	4
567	Spectroscopic ellipsometry study of the layer structure and impurity content in Er-doped nanocrystalline silicon thin films. Physica B: Condensed Matter, 2001, 308-310, 374-377.	1.3	4
568	Hyperfine Fields of 181Ta in UFe4Al8. Hyperfine Interactions, 2001, 136/137, 333-337.	0.2	4
569	Elemental characterisation of beryllium and electrical behaviour of their pebbles beds. Journal of Nuclear Materials, 2002, 307-311, 643-646.	1.3	4
570	Degradation of Structural and Optical Properties of InGaN/GaN Multiple Quantum Wells with Increasing Number of Wells. Physica Status Solidi C: Current Topics in Solid State Physics, 2003, 0, 302-306.	0.8	4
571	Characterization of FePt nanoparticles in FePt/C multilayers. Nuclear Instruments & Methods in Physics Research B, 2004, 219-220, 919-922.	0.6	4
572	Degradation of particle detectors based on a-Si:H by 1.5 Mev He4 and 1 MeV protons. Journal of Non-Crystalline Solids, 2004, 338-340, 814-817.	1.5	4
573	Structural and composition analysis of GaN films deposited by cyclic-PLD at different substrate temperatures. Sensors and Actuators A: Physical, 2005, 121, 131-135.	2.0	4
574	XRD analysis of strained Ge–SiGe heterostructures on relaxed SiGe graded buffers grown by hybrid epitaxy on Si(001) substrates. Materials Science and Engineering B: Solid-State Materials for Advanced Technology, 2005, 124-125, 123-126.	1.7	4
575	Stability of erbium and silver implanted in silica–titania sol–gel films. Nuclear Instruments & Methods in Physics Research B, 2005, 240, 415-419.	0.6	4
576	Beyond single scattering off flat samples. Nuclear Instruments & Methods in Physics Research B, 2005, 241, 316-320.	0.6	4

#	Article	IF	CITATIONS
577	Optical behaviour of Er doped rutile by ion implantation. Nuclear Instruments & Methods in Physics Research B, 2006, 250, 363-367.	0.6	4
578	The structure of crystallographic damage in GaN formed during rare earth ion implantation with and without an ultrathin AlN capping layer. Superlattices and Microstructures, 2006, 40, 300-305.	1.4	4
579	Lattice location of implanted As in ZnO. Superlattices and Microstructures, 2007, 42, 8-13.	1.4	4
580	Dual DC magnetron cathode co-deposition of (Al,Ti) and (Al,Ti,N) thin films with controlled depth composition. Vacuum, 2007, 81, 1503-1506.	1.6	4
581	Influence of the sol–gel growth parameters on the optical and structural properties on LiNbO3 samples. Materials Science and Engineering C, 2007, 27, 1065-1068.	3.8	4
582	Temperature behavior of damage in sapphire implanted with light ions. Nuclear Instruments & Methods in Physics Research B, 2009, 267, 1464-1467.	0.6	4
583	Stable In-defect complexes in GaN and AlN. Physica B: Condensed Matter, 2009, 404, 4866-4869.	1.3	4
584	High temperature annealing of Europium implanted AlN. Nuclear Instruments & Methods in Physics Research B, 2010, 268, 2907-2910.	0.6	4
585	Hydrogen retention in gallium samples exposed to ISTTOK plasmas. Fusion Engineering and Design, 2011, 86, 2458-2461.	1.0	4
586	Integration Of SIMS Into A General Purpose IBA Data Analysis Code. AIP Conference Proceedings, 2011, , .	0.3	4
587	Tuning the properties of Ge-quantum dots superlattices in amorphous silica matrix through deposition conditions. Journal of Applied Physics, 2012, 111, 074316.	1.1	4
588	Damage formation and recovery in Fe implanted 6H–SiC. Nuclear Instruments & Methods in Physics Research B, 2012, 286, 89-92.	0.6	4
589	Surface morphology, thermal and electrical conductivity of α-Al2O3 single crystals implanted with Au and Ag ions. Nuclear Instruments & Methods in Physics Research B, 2012, 286, 184-189.	0.6	4
590	Unintentional incorporation of H and related structural and freeâ€electron properties of <i>c</i> ―and <i>a</i> â€plane InN. Physica Status Solidi (A) Applications and Materials Science, 2012, 209, 91-94.	0.8	4
591	AIN content influence on the properties of AlxGa1â^'xN doped with Pr ions. Nuclear Instruments & Methods in Physics Research B, 2012, 273, 149-152.	0.6	4
592	Nanostructures and thin films of transparent conductive oxides studied by perturbed angular correlations. Physica Status Solidi (B): Basic Research, 2013, 250, 801-808.	0.7	4
593	Structural characterization of dual ion implantation in silicon. Nuclear Instruments & Methods in Physics Research B, 2015, 365, 39-43.	0.6	4
594	Retention behaviour of deuterium and helium in beryllium under single D+ and dual He+/D+ exposure. Fusion Engineering and Design, 2015, 98-99, 1362-1366.	1.0	4

#	Article	IF	CITATIONS
595	Studies of lithium deposition and D retention on tungsten samples exposed to Li-seeded plasmas in PISCES-A. Plasma Physics and Controlled Fusion, 2017, 59, 044006.	0.9	4
596	Structural and optical studies of aluminosilicate films doped with (Tb3+, Er3+)/Yb3+ by ion implantation. Nuclear Instruments & Methods in Physics Research B, 2019, 459, 71-75.	0.6	4
597	Stability of beryllium coatings deposited on carbon under annealing up to 1073 K. Fusion Engineering and Design, 2019, 146, 303-307.	1.0	4
598	Influence of Al/Si atomic ratio on optical and electrical properties of magnetron sputtered Al1-xSixOy coatings. Thin Solid Films, 2019, 669, 475-481.	0.8	4
599	Deuterium inventory determination in beryllium and mixed beryllium-carbon layers doped with oxygen. Fusion Engineering and Design, 2020, 150, 111365.	1.0	4
600	Lithium dilution in Li-Sn alloys. Nuclear Materials and Energy, 2020, 25, 100783.	0.6	4
601	Eu3+ optical activation engineering in Al Ga1-N nanowires for red solid-state nano-emitters. Applied Materials Today, 2021, 22, 100893.	2.3	4
602	Enhanced red emission from Eu-implanted ZnMgO layers and ZnO/ZnMgO quantum structures. Applied Physics Letters, 2021, 119, .	1.5	4
603	Nonpolar short-period ZnO/MgO superlattices: Radiative excitons analysis. Journal of Luminescence, 2021, 238, 118288.	1.5	4
604	Improvement of Mechanical Properties with Non-Equimolar CrNbTaVW High Entropy Alloy. Crystals, 2022, 12, 219.	1.0	4
605	Lattice site location and outdiffusion of mercury implanted in GaAs. Nuclear Instruments & Methods in Physics Research B, 1991, 59-60, 1090-1093.	0.6	3
606	Stability studies of Hg implanted YBa2Cu3O6+x. Nuclear Instruments & Methods in Physics Research B, 1999, 147, 244-248.	0.6	3
607	Stability and diffusion of Hg implanted YBa2Cu3O6+x. Nuclear Instruments & Methods in Physics Research B, 1999, 148, 807-812.	0.6	3
608	Strain and Compositional Analysis of InGaN/GaN Layers. Materials Research Society Symposia Proceedings, 2000, 639, 3521.	0.1	3
609	Structure determination of (Ti,Al)N/Mo multilayers. Thin Solid Films, 2000, 373, 287-292.	0.8	3
610	Annealing behavior and lattice site location of Er implanted InGaN. Nuclear Instruments & Methods in Physics Research B, 2003, 206, 1042-1046.	0.6	3
611	Characterization of the blue emission of Tm/Er co-implanted GaN. Materials Research Society Symposia Proceedings, 2005, 892, 544.	0.1	3
612	Compositional and structural characterisation of GaSb and GaInSb. Nuclear Instruments & Methods in Physics Research B, 2005, 240, 360-364.	0.6	3

#	Article	IF	CITATIONS
613	Comment on "Direct evidence of nanocluster-induced luminescence in InGaN epifilms―[Appl. Phys. Lett. 86, 021911 (2005)]. Applied Physics Letters, 2005, 87, 136101.	1.5	3
614	Structure and optical properties of sapphire implanted with boron at room temperature and 1000°C. Nuclear Instruments & Methods in Physics Research B, 2006, 250, 81-84.	0.6	3
615	Analysis of sol–gel silica–titania films doped with Ag and Er using artificial neural networks. Nuclear Instruments & Methods in Physics Research B, 2006, 249, 804-807.	0.6	3
616	Structural and Optical Characterization of Light Emitting InGaN/GaN Epitaxial Layers. Materials Science Forum, 2006, 514-516, 38-42.	0.3	3
617	Stability of GaN films under intense MeV He ion irradiation. Diamond and Related Materials, 2007, 16, 1437-1440.	1.8	3
618	Spectroscopic investigation of implanted epilayers of Tm3+:GaN. Journal of Luminescence, 2007, 122-123, 131-133.	1.5	3
619	A comparative investigation of the damage buildâ€up in GaN and Si during rare earth ion implantation. Physica Status Solidi (A) Applications and Materials Science, 2008, 205, 68-70.	0.8	3
620	Luminescence spectroscopy of Euâ€implanted zincblende GaN. Physica Status Solidi (B): Basic Research, 2008, 245, 170-173.	0.7	3
621	Optical and structural properties of Eu-implanted InxAl1â^'xN. Journal of Applied Physics, 2009, 106, .	1.1	3
622	Influence of Deposition Pressure on N-doped ZnO Films by RF Magnetron Sputtering. Journal of Nanoscience and Nanotechnology, 2010, 10, 2674-2678.	0.9	3
623	Effects of Mg-ion implantation in α-Al2O3 and α-Al2O3:Mg crystals: Electrical conductivity and electronic structure changes. Nuclear Instruments & Methods in Physics Research B, 2010, 268, 2874-2877.	0.6	3
624	Optical and Structural Properties of an Eu Implanted Gallium Nitride Quantum Dots/Aluminium Nitride Superlattice. Journal of Nanoscience and Nanotechnology, 2010, 10, 2473-2478.	0.9	3
625	Optical properties of AlN x O y thin films deposited by DC magnetron sputtering. , 2011, , .		3
626	The role of the annealing temperature on the optical and structural properties of Eu doped GaN/AlN QD. Optical Materials, 2011, 33, 1045-1049.	1.7	3
627	Unintentional incorporation of hydrogen in wurtzite InN with different surface orientations. Journal of Applied Physics, 2011, 110, .	1.1	3
628	Room Temperature Magnetic Response of Sputter Deposited TbDyFe Films as a Function of the Deposition Parameters. Journal of Nano Research, 0, 18-19, 235-239.	0.8	3
629	Stopping power of He, C and O in GaN. Nuclear Instruments & Methods in Physics Research B, 2012, 273, 26-29.	0.6	3
630	Status of the MARE Experiment. IEEE Transactions on Applied Superconductivity, 2013, 23, 2101204-2101204.	1.1	3

#	Article	IF	CITATIONS
631	Stopping power of 1H and 4He in lithium niobate. Nuclear Instruments & Methods in Physics Research B, 2014, 332, 330-333.	0.6	3
632	IBA study of SiGe/SiO2 nanostructured multilayers. Nuclear Instruments & Methods in Physics Research B, 2014, 331, 89-92.	0.6	3
633	Quantitative Chemical Mapping of InGaN Quantum Wells from Calibrated High-Angle Annular Dark Field Micrographs. Microscopy and Microanalysis, 2015, 21, 994-1005.	0.2	3
634	Composition measurement of epitaxial Sc _{<i>x</i>} Ga _{1â^'<i>x</i>} N films. Semiconductor Science and Technology, 2016, 31, 064002.	1.0	3
635	Micro-Opto-Electro-Mechanical Device Based on Flexible β-Ga ₂ O ₃ ÂMicro-Lamellas. ECS Journal of Solid State Science and Technology, 2019, 8, Q3235-Q3241.	0.9	3
636	Analysis of the outer divertor hot spot activity in the protection video camera recordings at JET. Fusion Engineering and Design, 2019, 139, 115-123.	1.0	3
637	Oxidation behaviour of neutron irradiated Be pebbles. Nuclear Materials and Energy, 2020, 23, 100748.	0.6	3
638	Deposition of Ti-Zr-O-N films by reactive magnetron sputtering of Zr target with Ti ribbons. Surface and Coatings Technology, 2021, 409, 126737.	2.2	3
639	Self-powered proton detectors based on GaN core–shell p–n microwires. Applied Physics Letters, 2021, 118, .	1.5	3
640	Advanced Monte Carlo Simulations for Ion-Channeling Studies of Complex Defects in Crystals. Springer Series in Materials Science, 2020, , 133-160.	0.4	3
641	Formation of AlxGa1â~'xSb films over GaSb substrates by Al diffusion. EPJ Applied Physics, 2004, 27, 423-426.	0.3	3
642	Rare Earth Ion Implantation in GaN: Damage Formation and Recovery. Acta Physica Polonica A, 2006, 110, 125-137.	0.2	3
643	Structural analysis of the ZnO/MgO superlattices on a-polar ZnO substrates grown by MBE. Applied Surface Science, 2022, 587, 152830.	3.1	3
644	Regrowth of indium-implanted (100), (110) and (111) silicon crystals studied with Rutherford backscattering and perturbed angular correlation techniques. Materials Science and Engineering B: Solid-State Materials for Advanced Technology, 1989, 4, 189-195.	1.7	2
645	Low temperature epitaxial regrowth of mercury implanted sapphire. Nuclear Instruments & Methods in Physics Research B, 1996, 120, 248-251.	0.6	2
646	Nuclear microbeam study of advanced materials for fusion reactor technology. Nuclear Instruments & Methods in Physics Research B, 1999, 158, 671-677.	0.6	2
647	Raman spectroscopy studies in InGaN/GaN wurtzite epitaxial films. Materials Research Society Symposia Proceedings, 2000, 639, 6101.	0.1	2
648	Indium Distribution within InxGa1?xN Epitaxial Layers: A Combined Resonant Raman Scattering and Rutherford Backscattering Study. Physica Status Solidi (B): Basic Research, 2001, 228, 173-177.	0.7	2

#	Article	IF	CITATIONS
649	Coherent amorphization of Ge/Si multilayers with ion beams. Nuclear Instruments & Methods in Physics Research B, 2001, 178, 279-282.	0.6	2
650	Structural Development in Hard Si-Based TiN Coatings as a Function of Temperature: A Comprehensive Study in Vacuum and in Air. Materials Science Forum, 2002, 383, 151-160.	0.3	2
651	Magnetic characterization of U/Co multilayers. Physica Status Solidi A, 2003, 196, 153-156.	1.7	2
652	The role of microstructure in luminescent properties of Er-doped nanocrystalline Si thin films. Physics of the Solid State, 2004, 46, 113-117.	0.2	2
653	Characterization of silicon carbide thin films and their use in colour sensor. Solar Energy Materials and Solar Cells, 2005, 87, 343-348.	3.0	2
654	Characterization and stability studies of titanium beryllides. Fusion Engineering and Design, 2005, 75-79, 759-763.	1.0	2
655	Influence of the Annealing Ambient on Structural and Optical Properties of Rare Earth Implanted GaN. Materials Research Society Symposia Proceedings, 2005, 892, 556.	0.1	2
656	Study of the oxygen role in the photoluminescence of erbium doped nanocrystalline silicon embedded in a silicon amorphous matrix. Journal of Non-Crystalline Solids, 2006, 352, 1148-1151.	1.5	2
657	Simulation of deep resonances in elastic backscattering data. Nuclear Instruments & Methods in Physics Research B, 2006, 249, 796-799.	0.6	2
658	Optical studies on a coherent InGaN/GaN layer. Superlattices and Microstructures, 2006, 40, 452-457.	1.4	2
659	Arsenic in ZnO and GaN: Substitutional Cation or Anion Sites?. Materials Research Society Symposia Proceedings, 2007, 994, 1.	0.1	2
660	Structural and Oxidation Studies of Titanium Beryllides. Nuclear Technology, 2007, 159, 233-237.	0.7	2
661	Implantation of nanoporous GaN with Eu ions. Nuclear Instruments & Methods in Physics Research B, 2007, 257, 328-331.	0.6	2
662	RBS analysis of InGaN/GaN quantum wells for hybrid structures with efficient Förster coupling. Nuclear Instruments & Methods in Physics Research B, 2008, 266, 1402-1406.	0.6	2
663	Electronic properties of Ge islands embedded in multilayer and superlattice structures. Thin Solid Films, 2008, 517, 303-305.	0.8	2
664	Features of the pulsed treatment of silicon layers implanted with erbium ions. Journal of Surface Investigation, 2009, 3, 604-607.	0.1	2
665	Annealing Ni nanocrystalline on WC–Co. Journal of Alloys and Compounds, 2009, 482, 131-136.	2.8	2
666	ZnO Thin Films Implanted with Al, Sb and P: Optical, Structural and Electrical Characterization. Journal of Nanoscience and Nanotechnology, 2009, 9, 3574-3577.	0.9	2

#	Article	IF	CITATIONS
667	Defect studies and optical activation of Yb doped GaN. Journal of Physics: Conference Series, 2010, 249, 012053.	0.3	2
668	Influence of temperature and plasma composition on deuterium retention in refractory metals. Nuclear Instruments & Methods in Physics Research B, 2010, 268, 2124-2128.	0.6	2
669	Carbon film growth and hydrogenic retention of tungsten exposed to carbon-seeded high density deuterium plasmas. Journal of Nuclear Materials, 2010, 396, 176-180.	1.3	2
670	Erbium-doped nanocrystalline silicon thin films produced by RF sputtering - annealing effect on the Er emission. Physica Status Solidi C: Current Topics in Solid State Physics, 2010, 7, NA-NA.	0.8	2
671	Stopping Power Of He, C And O In InN. , 2011, , .		2
672	CdTe nano-structures for photovoltaic devices. Nuclear Instruments & Methods in Physics Research B, 2013, 306, 218-221.	0.6	2
673	The influence of photon excitation and proton irradiation on the luminescence properties of yttria stabilized zirconia doped with praseodymium ions. Nuclear Instruments & Methods in Physics Research B, 2013, 306, 207-211.	0.6	2
674	Saturation of hydrogen retention in gallium samples exposed to tokamak ISTTOK plasmas. Journal of Nuclear Materials, 2013, 438, S992-S995.	1.3	2
675	Spectroscopy of radiation defects in rutile TiO ₂ . Physica Status Solidi (B): Basic Research, 2013, 250, 843-849.	0.7	2
676	The defect structure of sapphire produced by implantation of Zr and Zr plus O: threshold fluence for amorphization and optical properties. Physica Status Solidi C: Current Topics in Solid State Physics, 2013, 10, 202-207.	0.8	2
677	Laser-induced diffusion decomposition in Fe–V thin-film alloys. Applied Surface Science, 2015, 336, 380-384.	3.1	2
678	Ag y :TiN x thin films for dry biopotential electrodes: the effect of composition and structural changes on the electrical and mechanical behaviours. Applied Physics A: Materials Science and Processing, 2015, 119, 169-178.	1.1	2
679	Analysis of retained deuterium on Be-based films: Ion implantation vs. in-situ loading. Nuclear Materials and Energy, 2018, 17, 242-247.	0.6	2
680	Use of a Timepix position-sensitive detector for Rutherford backscattering spectrometry with channeling. Nuclear Instruments & Methods in Physics Research B, 2021, 499, 61-69.	0.6	2
681	Assessing material properties for fusion applications by ion beams. Nuclear Instruments & Methods in Physics Research B, 2017, 409, 255-258.	0.6	2
682	Confronting Vegard's rule in Ge _{1â^'x} Sn _x epilayers: from fundamentals to the effect of defects. Journal Physics D: Applied Physics, 2022, 55, 295301.	1.3	2
683	The lattice site of Au in Be after 24 h 197mHg isotope implantation and decay. Nuclear Instruments & Methods in Physics Research B, 1994, 85, 457-461.	0.6	1
684	Radiation damage annealing of Hg implanted InP. Nuclear Instruments & Methods in Physics Research B, 1996, 120, 244-247.	0.6	1

#	Article	IF	CITATIONS
685	Improving the Thermal Stability of Photoresist Films by Ion Beam Irradiation. Materials Research Society Symposia Proceedings, 1997, 504, 443.	0.1	1
686	Electrical conductivity in ion implanted TiO/sub 2/-single crystals. , 0, , .		1
687	Heavy ion implantation in GaN epilayers. Radiation Effects and Defects in Solids, 2001, 156, 267-272.	0.4	1
688	Study of solid-state reactions of SiC/SiCf composites using microbeams. Nuclear Instruments & Methods in Physics Research B, 2001, 181, 377-381.	0.6	1
689	Luminescence studies of Co implanted sapphires. Radiation Effects and Defects in Solids, 2002, 157, 1117-1122.	0.4	1
690	Surface quality studies of high-Tc superconductors of the Hg-, Tl- and HgxTl1â^'x-families: RBS and resonant C and O backscattering studies. Nuclear Instruments & Methods in Physics Research B, 2002, 190, 673-678.	0.6	1
691	Influence of crystals distribution on the photoluminescence properties of nanocrystalline silicon thin films. Microelectronics Journal, 2003, 34, 375-378.	1.1	1
692	Influence of ionizing radiation on the electrical behavior of a Be pebble bed. Fusion Engineering and Design, 2003, 69, 253-256.	1.0	1
693	Electron micro-probe analysis and cathodoluminescence spectroscopy of rare earth - implanted GaN. Materials Research Society Symposia Proceedings, 2003, 798, 466.	0.1	1
694	Stability and optical activity of Er implanted MgO. Nuclear Instruments & Methods in Physics Research B, 2004, 218, 128-132.	0.6	1
695	RBS analysis of AlGaSb thin films. Nuclear Instruments & Methods in Physics Research B, 2004, 219-220, 928-932.	0.6	1
696	Methods for the mitigation of the chemical reactivity of beryllium in steam. Journal of Nuclear Materials, 2004, 329-333, 1353-1356.	1.3	1
697	Rutherford backscattering and X-ray reflectivity analysis of tunnel barriers. Nuclear Instruments & Methods in Physics Research B, 2005, 240, 365-370.	0.6	1
698	Structure and role of ultrathin AlN layers for improving optical activation of rare earth implanted GaN. Physica Status Solidi (B): Basic Research, 2006, 243, 1541-1544.	0.7	1
699	Optical and structural behaviour of Mn implanted sapphire. Nuclear Instruments & Methods in Physics Research B, 2006, 250, 90-94.	0.6	1
700	Damage behaviour of GaAs/AlAs multilayer structures. Nuclear Instruments & Methods in Physics Research B, 2006, 249, 890-893.	0.6	1
701	UV-Raman scattering study of lattice recovery by thermal annealing of Eu+ -implanted GaN layers. Superlattices and Microstructures, 2006, 40, 440-444.	1.4	1
702	Phase Separation on GalnAsSb Films for Thermophotovoltaic Devices. Materials Science Forum, 2006, 514-516, 447-451.	0.3	1

#	Article	IF	CITATIONS
703	Hardware and Software Improvements in the Hotbird. Materials Science Forum, 2006, 514-516, 1678-1681.	0.3	1
704	Effect of the Matrix on the 1.5μm Photoluminescence of Er-Doped Silicon Quantum Dots. Materials Science Forum, 2006, 514-516, 1116-1120.	0.3	1
705	Lithium ion implantation and annealing of MgO single crystals. Nuclear Instruments & Methods in Physics Research B, 2007, 257, 558-562.	0.6	1
706	Radiation-induced structural transformations in a silicon layer of SOI. Physica Status Solidi (A) Applications and Materials Science, 2007, 204, 2645-2650.	0.8	1
707	Anisotropy effects on the formation of new phases in α-Al2O3 by high fluence Zn implantation. Nuclear Instruments & Methods in Physics Research B, 2008, 266, 3129-3132.	0.6	1
708	Role of the oxygen partial pressure on the properties of undoped tin oxide films deposited at low temperature. Physica Status Solidi (A) Applications and Materials Science, 2008, 205, 1957-1960.	0.8	1
709	Structural study of the oxidation process and stability of NbOxNy coatings. Nuclear Instruments & Methods in Physics Research B, 2008, 266, 4927-4932.	0.6	1
710	W-Diamond/Cu-Diamond nanostructured composites for fusion devices. Materials Research Society Symposia Proceedings, 2008, 1125, 1.	0.1	1
711	The Structure of Sapphire Implanted with Carbon at Room Temperature and 1000° C. , 2009, , .		1
712	Lattice location and annealing studies of Hf implanted CaF2. Nuclear Instruments & Methods in Physics Research B, 2009, 267, 1472-1475.	0.6	1
713	Defects in Irradiated ZnO Thin Films Studied by Photoluminescence and Photoconductivity. Materials Research Society Symposia Proceedings, 2010, 1268, 1.	0.1	1
714	Improved Route for the Synthesis of Colloidal NaYF ₄ Nanocrystals and Electron Spin Resonance of Gd ³⁺ Local Probe. Journal of Nanoscience and Nanotechnology, 2010, 10, 5708-5714.	0.9	1
715	Electroless plating of Au, Pt, or Ru thin film layer on CdZnTe. , 2011, , .		1
716	Materials research under ITER-like divertor conditions at FOM Rijnhuizen. Journal of Nuclear Materials, 2011, 417, 457-462.	1.3	1
717	A Double Scattering Analytical Model For Elastic Recoil Detection Analysis. , 2011, , .		1
718	Hydrogen In Group-III Nitrides: An Ion Beam Analysis Study. , 2011, , .		1
719	Wettability and Nanotribological Response of Silicon Surfaces Functionalized by Ion Implantation. Materials Science Forum, 0, 730-732, 257-262.	0.3	1
720	Ion beams as a tool for the characterization of near-pseudomorphic CdZnO epilayers. , 2012, , .		1

#	Article	lF	CITATIONS
721	Electronic structure of ytterbium-implanted GaN at ambient and high pressure: experimental and crystal field studies. Journal of Physics Condensed Matter, 2012, 24, 095803.	0.7	1
722	Characterization of nanostructured HfO2 films using RBS and PAC. Nuclear Instruments & Methods in Physics Research B, 2012, 273, 195-198.	0.6	1
723	Influence of RF-sputtering power on formation of vertically stacked Si _{1â°'<i>x</i>} Ge _{<i>x</i>} nanocrystals between ultra-thin amorphous Al ₂ O ₃ layers: structural and photoluminescence properties. Journal Physics D: Applied Physics. 2013, 46, 385301.	1.3	1
724	Local deposition of 13C tracer in the JET MKII-HD divertor. Journal of Nuclear Materials, 2013, 438, S762-S765.	1.3	1
725	Thermal Properties of Holmium-Implanted Gold Films. Journal of Low Temperature Physics, 2014, 176, 979-985.	0.6	1
726	Nanoscale triboactivity of functionalized c-Si surfaces by Fe ⁺ ion implantation. Journal of Physics Condensed Matter, 2016, 28, 134003.	0.7	1
727	Anisotropy of electrical conductivity in dc due to intrinsic defect formation in α-Al2O3 single crystal implanted with Mg ions. Nuclear Instruments & Methods in Physics Research B, 2016, 379, 91-94.	0.6	1
728	Study of nuclear reactions producing ³⁶ Cl by micro-AMS. Journal of Physics: Conference Series, 2016, 665, 012077.	0.3	1
729	Quantum well intermixing and radiation effects in InGaN/GaN multi quantum wells. , 2016, , .		1
730	Helium and deuterium irradiation effects in tungsten-based materials with titanium. Surface and Coatings Technology, 2018, 355, 143-147.	2.2	1
731	In-situ XRD vs ex-situ vacuum annealing of tantalum oxynitride thin films: Assessments on the structural evolution. Applied Surface Science, 2018, 438, 14-19.	3.1	1
732	Luminescence properties of MOCVD grown Al0.2Ga0.8N layers implanted with Tb. Journal of Luminescence, 2019, 210, 413-424.	1.5	1
733	Estimating the uncertainties of strain and damage analysis by X-ray diffraction in ion implanted MoO3. Nuclear Instruments & Methods in Physics Research B, 2020, 478, 290-296.	0.6	1
734	Ion beam induced current analysis in GaN microwires. EPJ Web of Conferences, 2020, 233, 05001.	0.1	1
735	Electrical, optical and photoconductive properties of Sn-doped indium sulfofluoride thin films. Materials Science in Semiconductor Processing, 2021, 121, 105349.	1.9	1
736	Rutherford Backscattering and Photoluminescence Studies of Erbium Implanted GaAs. Materials Research Society Symposia Proceedings, 1996, 422, 173.	0.1	0
737	RBS Lattice Site Location and Damage Recovery Studies In GaN. Materials Research Society Symposia Proceedings, 1998, 537, 1.	0.1	0
738	Characterisation of YBaCuO-PrBaCuO Multilayers Grown by Pulsed Injection MO-CVD. Journal of Low Temperature Physics, 1999, 117, 657-661.	0.6	0

#	Article	IF	CITATIONS
739	Optical Characterization of AlGaN/GaN MQW's. Materials Research Society Symposia Proceedings, 2000, 639, 6211.	0.1	0
740	Mechanical and Adhesion Behaviours of Superhard (Ti,Si,Al)N Nanocomposite Films Grown by Reactive Magnetron Sputtering. Key Engineering Materials, 2002, 230-232, 185-188.	0.4	0
741	Lattice Site Location Studies of Rare-Earths Implanted in ZnO Single-Crystals. Materials Research Society Symposia Proceedings, 2002, 744, 1.	0.1	0
742	High temperature chemical compatibility between SiC composites and Be pebbles. Nuclear Instruments & Methods in Physics Research B, 2003, 210, 495-500.	0.6	0
743	Structural characterisation of SiC/SiCf composites exposed to chemical interaction with Be at high temperature. Fusion Engineering and Design, 2003, 69, 221-226.	1.0	0
744	Ion beam studies of single crystalline manganite thin films. Nuclear Instruments & Methods in Physics Research B, 2004, 219-220, 933-937.	0.6	0
745	Analysis of nanolayered samples with a 4He beam. Nuclear Instruments & Methods in Physics Research B, 2005, 241, 361-364.	0.6	0
746	Site location and optical properties of Eu implanted sapphire. Nuclear Instruments & Methods in Physics Research B, 2005, 240, 409-414.	0.6	0
747	A microspectroscopic study of cap damage in annealed RE-doped AlN-capped GaN. Materials Research Society Symposia Proceedings, 2005, 892, 568.	0.1	0
748	Optical properties of Er3++ Yb3+doped gallium nitride layers. , 2006, , .		0
749	RBS and XRD analysis of SiGe/Ge heterostructures for p-HMOS applications. Nuclear Instruments & Methods in Physics Research B, 2006, 249, 878-881.	0.6	0
750	Characterization of Nickel Implanted α-Al ₂ O ₃ . Materials Science Forum, 2006, 514-516, 348-352.	0.3	0
751	X-Ray Diffraction Study of Ordered Antiferromagnets for Tunnel Junctions. Materials Science Forum, 2006, 514-516, 314-318.	0.3	0
752	Ion Beam Analysis of Ge/Si Dots Grown on Ultrathin SiO ₂ Interlayers. Materials Science Forum, 2006, 514-516, 1121-1124.	0.3	0
753	OPTICAL AND STRUCTURAL ANALYSIS OF Ge/Si QUANTUM DOTS GROWN ON A Si(001) SURFACE COVERED WITH A SiO2 SUB-MONOLAYER. International Journal of Nanoscience, 2007, 06, 245-248.	0.4	0
754	lon implantation and ion beam analysis of MOD deposited oxide films. Nuclear Instruments & Methods in Physics Research B, 2007, 261, 456-460.	0.6	0
755	Luminescence and vibrational properties of erbium-implanted nanoporous GaN. Physica Status Solidi C: Current Topics in Solid State Physics, 2008, 5, 1753-1755.	0.8	0
756	Ion beam studies of InAs/GaAs self assembled quantum dots. Nuclear Instruments & Methods in Physics Research B, 2008, 266, 1439-1442.	0.6	0

#	Article	IF	CITATIONS
757	Structural and Mechanical Properties of AZOY Thin Films Deposited on Flexible Substrates. Materials Science Forum, 0, 587-588, 834-838.	0.3	0
758	Effects of hydrogen permeation on W, Mo and Cu Langmuir probes at ISTTOK. Materials Research Society Symposia Proceedings, 2008, 1125, 1.	0.1	0
759	Microstructure characterization of ODS-RAFM steels. Materials Research Society Symposia Proceedings, 2008, 1125, 1.	0.1	0
760	Study of SiGe Alloys with Different Germanium Concentrations Implanted with Mn and As Ions. Materials Science Forum, 0, 587-588, 298-302.	0.3	0
761	Nanoscale Materials Defect Characterisation. Particle Acceleration and Detection, 2009, , 185-204.	0.3	0
762	Structural and photoluminescence studies of erbiumâ€implanted nanocrystalline silicon thin films. Physica Status Solidi (A) Applications and Materials Science, 2009, 206, 2161-2165.	0.8	0
763	Ion Beam Analysis of Iridium-Based TES for Microcalorimeter Detectors. , 2009, , .		0
764	Total reflectance and Raman studies in Al _y In _x Ga _{1â€xâ€y} N epitaxial layers. Physica Status Solidi C: Current Topics in Solid State Physics, 2010, 7, 56-59.	0.8	0
765	Growth and characterization of Mnâ€doped ZnO/TiO ₂ multilayer nanostructures grown by pulsed laser deposition. Physica Status Solidi C: Current Topics in Solid State Physics, 2010, 7, 2724-2726.	0.8	0
766	Mass spectrometry improvement on an high current ion implanter. Nuclear Instruments & Methods in Physics Research B, 2011, 269, 3222-3225.	0.6	0
767	Optimization Of A Mass Spectrometry Process. , 2011, , .		0
768	Damage formation in GaN under medium energy range implantation of rare earth ions: a combined TEM, XRD and RBS/C investigation. Materials Research Society Symposia Proceedings, 2011, 1342, 35.	0.1	0
769	Structural and Electrical Properties of Nanostructured Ba _{0.8} Sr _{0.2} TiO ₃ Films Deposited by Pulsed Laser Deposition. Journal of Nano Research, 2012, 18-19, 299-306.	0.8	0
770	Carbon Deposition on Beryllium Substrates and Subsequent Delamination. Materials Science Forum, 2012, 730-732, 179-184.	0.3	0
771	Editorial – 13th ICNMTA 2012. Nuclear Instruments & Methods in Physics Research B, 2013, 306, 1-2.	0.6	0
772	On the origin of strain relaxation in epitaxial CdZnO layers. , 2013, , .		0
773	Growth of mixed materials in the Be/W/O system in fusion devices. Microscopy and Microanalysis, 2015, 21, 94-95.	0.2	0
774	W-Ta Composites Consolidated by Spark Plasma Sintering. Microscopy and Microanalysis, 2015, 21, 27-28.	0.2	0

#	Article	IF	CITATIONS
775	Formation of metastable phases in Zr-ion-irradiated Al2O3 upon thermal annealing. Journal of Electron Microscopy, 2017, 66, 388-396.	0.9	0
776	Nanostructured c-Si surfaces obtained by sequential ion implantation of C+ and Ti+: Tribophysical and structural characterization. Nuclear Instruments & Methods in Physics Research B, 2020, 471, 69-75.	0.6	0
777	Ion beam analysis of Li-Sn alloys for fusion applications. Nuclear Instruments & Methods in Physics Research B, 2021, 486, 55-62.	0.6	0
778	Recent Emission Channeling Studies in Wide Band Gap Semiconductors. , 2005, , 792-801.		0
779	Enhancement of Erbium Incorporation with Implantation into Nanoporous GaN. , 2008, , .		0
780	Temperature dependence of the electric field gradient in GaN measured with the PAC-probe 181Hf. , 2008, , 217-223.		0
781	Box 6: Nanoscale Defects. Particle Acceleration and Detection, 2009, , 205-210.	0.3	0
782	Computer Control of a 3 MV Van de Graaff Accelerator. Metrology and Measurement Systems, 2010, 17, 415-425.	1.4	0
783	Incorporation and stability of erbium in sapphire by ion implantation. , 1996, , 429-432.		0
784	Corrosion Behavior of Titanium Oxynitrided by Diffusion and Magnetron Sputtering Methods in Physiological Solution. Materials Performance and Characterization, 2017, 6, 594-606.	0.2	0
785	PAC Studies of Implanted 111Ag in Single-Crystalline ZnO. , 2005, , 395-400.		0